ESTIMATING THE UNDRAINED STRENGTH OF SAND: A THEORETICAL FRAMEWORK

by

Catherine E. Fear and Peter K. Robertson

Geotechnical Group
Department of Civil Engineering
220 Civil/Electrical Engineering Building
University of Alberta
Edmonton, Alberta
CANADA, T6G 2G7

Tel: (403) 492-5106
Fax: (403) 492-8198

Submitted to

Canadian Geotechnical Journal

May 31, 1994

ABSTRACT

A framework for estimating the ultimate undrained steady state shear strength of sand (S_u) from *in-situ* tests, which combines critical state soil mechanics theory and shear wave velocity measurements, is presented. Samples of a given sand at a constant void ratio will reach the same S_u, when loaded undrained, despite the magnitude of the initial effective confining stresses. Unique S_u/p' or S_u/σ_v' ratios exist for a particular sand only if state parameter is constant throughout the deposit. Normalized shear wave velocity, V_{s1}, can be correlated with void ratio and is therefore used to estimate S_u for a given initial state. A simple sensitivity analysis demonstrates the impact of uncertainty in the V_{s1}-void ratio correlation on the estimated values of S_u. V_{s1} is converted to equivalent values of SPT $(N_1)_{60}$ and CPT q_{c1} and the results are compared to the current methods of estimating S_u.

Key words: undrained strength, in-situ, liquefaction.

INTRODUCTION

Stability analyses of sand loaded under undrained conditions, such as post-liquefaction conditions, require a knowledge of the ultimate undrained steady state shear strength (S_u) that the sand will possess. Provided that liquefaction will be triggered in a sandy slope, the great difficulty lies in deciding what value of S_u will best represent the particular conditions in the field. Current practice makes use of correlations between S_u and Standard Penetration Test (SPT) or Cone Penetration Test (CPT) resistance (Seed and Harder 1990; Robertson 1990; Stark and Mesri 1992).

This study presents a framework for estimating S_u, combining critical state soil mechanics and shear wave velocity measurements, assuming undrained loading with no pore pressure redistribution. The shear wave velocity measurements can also be converted to equivalent SPT and CPT penetration resistance. As a result, the uniqueness of each of the current empirical methods for estimating the S_u using field penetration tests is critically examined and the factors that play a major role in the potential correlations between S_u and penetration resistance are investigated.

CURRENT METHODS FOR ESTIMATING S_u USING PENETRATION TESTS

Seed and Harder (1990) present an empirical correlation, based on the original work by Seed (1987), which draws on 17 case histories and provides a relationship between S_u and equivalent normalized Standard Penetration Test (SPT) resistance, $(N_1)_{60}$, in clean sand. This relationship consists of a lower bound and an upper bound. These bounds present a dilemma to the geotechnical engineer. It is not uncommon to find that the upper bound line will result in an acceptable factor of safety whereas the lower bound line will suggest a potentially unstable condition. Conservative practice leads engineers to often use the lower bound line which may result in unnecessary expenditures.

Stark and Mesri (1992) provide an alternative approach to estimating S_u, and present a relationship between undrained strength ratio and equivalent $(N_1)_{60}$ in clean sand. The undrained strength ratio is defined as the mobilized S_u, divided by the initial effective vertical stress, σ_v'. This relationship is based on the 17 case histories used by Seed and Harder (1990) together with 3 additional case histories. The Stark and Mesri (1992) relationship also consists of lower and upper bound lines and thus, in design, will present the same problems as the plot by Seed and Harder (1990). The work by Stark and Mesri followed the approach taken by Jefferies *et al* (1990), which suggested that the shear strength ratio was a function of normalized CPT resistance. This idea was based on the view that shear strength ratio is a function of state parameter (Ψ) and the previous work by Been and Jefferies (1986 and 1987) which proposed that state parameter was a function of normalized CPT resistance.

Robertson (1990) presents a review of the relationship between S_u and normalized penetration resistance using relative density correlations with SPT $(N_1)_{60}$, correlations between normalized CPT q_{c1} and SPT $(N_1)_{60}$, published data on steady state relationships, field studies and large calibration chamber test results. Upon comparison of these results for four different sands with the upper and lower bound lines from the early work by Seed (1987), Robertson found that Ottawa sand appeared to provide the minimum steady state strength correlation and that the correlation by Seed (1987) represented a conservative lower bound correlation, especially at large values of $(N_1)_{60}$. The other sands that were studied (Monterey, Ticino and Hilton Mines) all possessed much higher steady state strengths at a given value of penetration resistance than the Seed (1987) correlation would suggest, thus indicating that there appears to be no unique relationship between S_u and penetration resistance for all sands.

Robertson (1990) also investigated the correlation between normalized ultimate undrained strength (S_u/p') and normalized CPT resistance $(q_c-p)/p'$, based on state parameter, as suggested by Been and Jefferies (1985). Again, it was found that there was no unique relationship for all sands, with

Ottawa sand representing the minimum relationship when compared with the other sands (Reid Bedford, Hilton Mines, Oilsand, Ticino and Monterey). Robertson (1990) recognized that these correlations were approximate in nature due to limited test data, but the results clearly suggested the lack of a unique relationship.

The approach taken at Duncan Dam (B.C. Hydro, 1993) to estimate S_u was an alternative to the *in-situ* penetration methods discussed above. High quality undisturbed samples of sand were obtained at Duncan Dam using ground freezing and subsequent coring. These undisturbed samples were then tested in the laboratory to directly determine S_u of the sand. Although attractive, this approach can be expensive and limited to large projects.

PROPOSED FRAMEWORK FOR ESTIMATING S_u BASED ON SHEAR WAVE VELOCITY MEASUREMENTS

Determining S_u from critical state soil mechanics

The collapse surface approach (Sladen *et al* 1985) to liquefaction analysis resides within a critical state soil mechanics framework. Within this framework, it is possible to calculate the value of S_u that a soil will reach when loaded in undrained shear (i.e. no change in void ratio), given the initial void ratio and stress state of the soil. The ultimate steady state line (SSL) for a given sand can be plotted in p'-q-e space (see Figure 1a), where e is void ratio and p' and q are defined as follows:

$$p' = \frac{1}{3}(\sigma_1' + 2\,\sigma_3') \qquad [1]$$

$$q = \sigma_1' - \sigma_3' \qquad [2]$$

When this line in p'-q-e space is projected onto the e-p' plane and the p' axis is plotted on a logarithmic scale, the SSL can be approximated as a straight line over a given stress range (see Figure 1b). The SSL in the e-p' plane can be defined by two parameters, Γ and λ. Γ is the intercept of the SSL at p'=1 kPa and λ is the slope of the SSL. Note that this definition of Γ is a void ratio not a specific volume. It is also important to note whether λ is defined with p' plotted on a natural logarithm scale (noted here as λ_{ln}) or a logarithm base 10 scale (noted here as λ_{log}). The ratio of λ_{ln} to λ_{log} is approximately 0.434. Therefore, it is essential, when comparing values of Γ and λ for different sands, to ensure that they are defined in the same way. In this paper, λ_{ln} will be used, such that the SSL in e-*ln* p' space is defined as follows:

$$e = \Gamma - \lambda_{ln}\, ln\,(p') \quad \text{or} \quad p' = \exp\left(\frac{\Gamma - e}{\lambda_{ln}}\right) \qquad [3]$$

A sand which has an initial state given by (p', q, e) and is loaded in undrained shear (i.e. no change in void ratio) will reach the same S_u as the point on the SSL with the same void ratio (see Figure 1). At any point (p'_{ss}, q_{ss}, e) along the SSL, S_u, can be determined as follows:

$$S_u = \frac{1}{2} q_{ss} \qquad [4]$$

Along the SSL, q and p' are related as follows:

$$q_{ss} = M \bullet p_{ss}' \qquad [5]$$

where:

$$M = \frac{6 \sin \phi'_{ss}}{3 - \sin \phi'_{ss}} \quad \text{(in triaxial compression)} \qquad [6]$$

$$p_{ss}' = \frac{p'}{\exp\left(\frac{\Psi}{\lambda_{ln}}\right)} \qquad [7]$$

ϕ'_{ss} = the steady state friction angle

λ_{ln} = slope of the SSL in e-*ln* p' space

Ψ= state parameter = e - e_{ss} (Been and Jefferies 1985) [8]

e = initial void ratio

e_{ss} = void ratio of the point on the SSL with the same p' as the initial state

Combining equations 3 to 7 results in the following equation for S_u:

$$S_u = \frac{1}{2} M \left(\frac{p'}{\exp\left(\frac{\Psi}{\lambda_{ln}}\right)} \right) \quad [9]$$

Thus, it can be seen that for a certain sand (i.e. constant M and λ_{ln}), S_u is a function of both state parameter, Ψ, and p'. Rearranging equation 9 produces the following equation for S_u/p':

$$\frac{S_u}{p'} = \frac{1}{2} M \exp\left(-\frac{\Psi}{\lambda_{ln}}\right) \quad [10]$$

Thus, for a given sand, the ultimate undrained steady state shear strength ratio is solely a function of state parameter. Hence, by determining the state parameter, S_u/p' can be evaluated at a specific location in the ground. The maximum value of S_u/p' for a contractant soil (i.e. $\Psi \geq 0$) occurs when Ψ=0 and has a value equal to 0.5 M. By determining p' as well as Ψ, S_u can be calculated.

For a given sand, a constant S_u/p' ratio applies only if the *in-situ* consolidation line is parallel to the SSL on an e-*ln* p' plot, resulting in a constant state parameter. In this sense, sand differs from clay. For clay, it is reasonable to assume that the virgin compression line (i.e. normally consolidated clay) and the SSL are relatively straight and parallel in e-*ln* p' space (Wood 1990). All points on the virgin compression line have the same state parameter and, therefore, a constant value of S_u/p' can be used for a particular normally consolidated clay. Sand, however, can be

deposited in numerous ways, each producing a different consolidation line which may or may not be parallel to the SSL.

On a site-specific basis, a constant S_u/p' ratio can be used only if the combinations of void ratio and stress at all points in the ground produce a constant state parameter. If state parameter is not constant at all points in the ground as a result of different depositional processes, then it is incorrect to assume a constant value of S_u/p' for a deposit. Experience with reconstituted sand samples in the laboratory indicates that the consolidation line for very loose sands can be approximately parallel to the SSL (Cunning 1994). Therefore, a constant value of S_u/p' may be reasonable for very loose sands.

Estimating soil state from shear wave velocity measurements

Been and Jefferies (1986, 1987) suggested using normalized CPT resistance to determine state parameter. This approach, which requires large calibration chamber testing, will be reviewed later in the paper. The disadvantages of this method are that large calibration chamber tests are expensive and are subject to boundary effects; in addition, there is uncertainty over the normalization techniques for penetration resistance (Sladen 1989) and extrapolation into the loose range.

An alternative approach is to make use of the relationship between shear wave velocity (V_s) and state parameter developed by Robertson *et al* (1994). Shear wave velocity is an attractive parameter to use because it can easily be measured in both the field and the laboratory. No corrections are required for boundary effects and the normalization procedure for overburden stress is developed directly. Shear wave velocity is predominantly a function of the void ratio and effective stress conditions in the soil. Soil compressibility, which can have a large effect on SPT and CPT penetration resistance, has no effect on shear wave velocity. Fabric, aging and

cementation of the soil will also affect shear wave velocity measurements. However, the primary goal of this study is to estimate S_u in loose sands which may be subject to flow liquefaction. Such sands are likely young, uncemented sands; thus, aging and cementation are unlikely to be of major concern. Fabric can influence V_s; however, there is evidence to suggest that fabric has little effect in very loose sands (Robertson *et al* 1994).

State parameter, as defined by Been and Jefferies (1985) in equation 8, is the difference between the current void ratio and the void ratio of the point on the SSL with the same mean normal effective stress (p') as the current point. The latter can be defined as follows (see Figure 1):

$$e_{ss} = \Gamma - \lambda_{ln} \bullet ln\,(p') \qquad [11]$$

Sasitharan (1994) showed that the current void ratio can be estimated by measuring shear wave velocity and using the relationship:

$$e = \frac{A}{B} - \frac{V_s\,(Pa)^{(na+nb)}}{B(\sigma'_a)^{na}(\sigma'_p)^{nb}} \qquad [12]$$

where:

V_s = shear wave velocity, in m/s

σ'_a = the effective stress in the direction of wave propagation, in kPa

σ'_p = the effective stress in the direction of particle motion, in kPa

A and B = constants for a given sand, both in m/s

na and nb = stress exponents; typically, na = nb = 0.125

Combining equations 8, 11 and 12 results in the following equation for state parameter, as given by Sasitharan (1994):

$$\Psi = C - V_s\Psi \quad [13]$$

where:

$$C = \frac{A}{B} - \Gamma \quad [14]$$

$$V_s\Psi = \left(\frac{V_s\,(P_a)^{na+nb}}{B\,(\sigma_a')^{na}\,(\sigma_p')^{nb}} - \lambda_{1n}\, ln\, p' \right) \quad [15]$$

Making the following substitutions:

$$\sigma_a' = \sigma_h' = K_o \bullet \sigma_v' \quad [16]$$

$$\sigma_p' = \sigma_v' \quad [17]$$

$$p' = \frac{1}{3}(\sigma_1' + 2\sigma_3') = \frac{1}{3}(\sigma_v' + 2\sigma_h') = \frac{\sigma_v'}{3}(1 + 2K_o) \quad [18]$$

results in the following equation relating state parameter to shear wave velocity:

$$\Psi = \left(\frac{A}{B} - \Gamma \right) - \left(\frac{V_s\,(P_a)^{na+nb}}{B\,(\sigma_v')^{na+nb}\,(K_o)^{na}} - \lambda_{1n}\, ln \left[\frac{\sigma_v'}{3}(1 + 2K_o) \right] \right) \quad [19]$$

From this equation, it can be seen that state parameter is a function of soil type (A, B, Γ and λ_{1n}), K_o, and shear wave velocity, V_s.

Measured values of shear wave velocity, V_s, are usually corrected to normalized shear wave velocity, V_{s1}, to account for overburden stress, using the following equation:

$$V_{s1} = V_s \left(\frac{P_a}{\sigma_v'} \right)^{na+nb} \quad [20]$$

where P_a = 100 kPa and na=nb=0.125, typically

Substituting equation 20 into equation 19 results in the following equation relating state parameter to V_{s1}:

$$\Psi = \left(\frac{A}{B} - \Gamma\right) - \left(\frac{V_{s1}}{B\,(K_o)^{na}} - \lambda_{1n}\, ln\left[\frac{\sigma_v'}{3}(1 + 2K_o)\right]\right) \qquad [21]$$

Estimating S_u from shear wave velocity measurements

Combining equation 9, which expresses S_u as a function of Ψ, with equation 21, which expresses Ψ as a function of V_{s1}, results in the following equation relating S_u to V_{s1}:

$$S_u = \frac{M}{2}\exp\left[\frac{1}{\lambda_{1n}}\left(\frac{V_{s1}}{B\,(K_o)^{na}} - \left(\frac{A}{B} - \Gamma\right)\right)\right] \qquad \text{(kPa)} \qquad [22]$$

where V_{s1} is in m/s and λ_{1n} has units of $\frac{1}{ln(\text{kPa})}$

Similarly, combining equations 10 and 21 results in the following equation relating S_u/p' to V_{s1}:

$$\frac{S_u}{p'} = \frac{M}{2}\,\frac{\exp\left[\frac{V_{s1}}{B\,(K_o)^{na}} - \lambda_{1n}\, ln\left(\frac{\sigma_v'}{3}(1 + 2K_o)\right)\right]}{\exp\left(\frac{A}{B} - \Gamma\right)} \qquad [23]$$

Replacing p' in the left side of equation 23 by the expression given in equation 18 results in a similar equation relating S_u/σ_v' to shear wave velocity:

$$\frac{S_u}{\sigma_v'} = \frac{M}{6}\left(\frac{\exp\left[\frac{V_{s1}}{B\,(K_o)^{na}} - \lambda_{1n}\, ln\left(\frac{\sigma_v'}{3}(1 + 2K_o)\right)\right]}{\exp\left(\frac{A}{B} - \Gamma\right)}\right)(1 + 2K_o) \qquad [24]$$

Examining equation 22, it is clear that for a given material (i.e. A, B, na, M, Γ and λ_{1n} are constants) and for a given K_o, S_u is a uniquely a function of V_{s1}. Therefore, if the steady state parameters M, Γ and λ_{1n} have been carefully determined, A, B and na have been evaluated, and a good estimate of K_o can be made, measuring shear wave velocity and converting it to V_{s1} can be used to directly determine S_u in a given sand. However, equations 23 and 24 show that neither S_u/p' nor S_u/σ_v' is a unique function of V_{s1}, even for a given material and K_o. Rather, S_u/p' and S_u/σ_v' remain a function of σ_v' as well. Thus, one would expect to get a series of relationships between S_u/p' and V_{s1} for different values of σ_v'.

APPLICATION OF THE PROPOSED APPROACH FOR TWO SANDS

Test program

Ottawa sand and a compressible tailings sand from Alaska (herein referred to as Alaska sand) were selected for use in this study as they appeared to represent two extremes encompassing most sands that could be encountered in practice. Laboratory data were available for both sands and field data (SPT, CPT and V_s logs) were available for Alaska sand. Ottawa sand is a clean, uniform, subrounded quartz sand that is relatively incompressible. Alaska sand contains approximately 30% fines (passing the No. 200 sieve), composed of a large amount of carbonate shell material which increases the compressibility of the sand significantly.

Laboratory testing has been carried out at the University of Alberta on both sands (Sasitharan 1994; Cunning 1994) in the form of triaxial compression tests with shear wave velocity measurements. The material properties for Ottawa and Alaska sand are given in Table 1, together with the values for other sands tabulated by Sasitharan *et al* (1993). Note that the parameters Γ and λ_{1n} are significantly different for Ottawa and Alaska sand, reflecting the major differences in fabric and compressibility in hydrostatic loading (p'), respectively. Figure 2(a) presents the ultimate

SSLs for both Ottawa sand and Alaska sand on an e-*ln* p' plot, relative to the ultimate SSLs for the other sands from Sasitharan *et al* (1993). It can be seen that Alaska sand clearly represents an upper bound SSL up to a p' approximately equal to 55 kPa (at which point, Lornex sand becomes the upper bound), while Ottawa sand is one of the lower bound SSL's.

Pitman (1993) and Skirrow (1994) studied the effects of adding varying amounts of kaolinite fines to clean Ottawa sand on the location of the SSL and on the relationship between V_{s1} and void ratio. Table 1 also contains the material properties for clean Ottawa sand with added fines contents of 5%, 7.5% and 10% from Skirrow (1994) and for kaolin (i.e. fines content of 100%), based on Atkinson (1993). Skirrow (1994) found that the SSL became steeper (i.e. larger λ_{1n}) as the fines content was increased from 0% to 10%, but that the value of Γ remained relatively similar to that for clean Ottawa sand. This can be seen in Figure 2(b). Pitman (1993) noted that the position of the SSL for a particular initial stress (p'=350 kPa) moved downwards as the percentage of fines added was increased up to 20%; however, the SSL moved back upwards as the fines content was increased above 20%. The position of the SSL for kaolin (100% fines) in Figure 2(b), well above that for Alaska sand, is consistent with this finding.

The values of A and B for Ottawa and Alaska sand, given in Table 1, are based on the typical values of the stress exponents na and nb in equation 12 being both equal to 0.125 for a combined total of 0.250. However, it was found, when testing these two sands (Cunning 1993), that the best fit values for the combined total of na plus nb were 0.266 for Ottawa sand and 0.260 for Alaska sand. Although it appears that the stress exponents are dependent on the type of sand, this study adopted the historical value for (na + nb) of 0.25 as being a generalized value that could be applied to all sands. This was divided equally with na and nb assigned equal values of 0.125.

The values of A and B were not available for the various sands tabulated by Sasitharan *et al* (1993), the Ottawa sand with added fines, or for kaolin. However, it has been shown (Cunning

1994) that most sands tend to fall within a certain band on a V_{s1}-e plot. This band has average values of A and B equal to 363 m/s (range = 340 to 380 m/s) and 235 m/s, respectively, for na and nb both equal to 0.125, as discussed above. In this study, these global values of A and B were applied to the other sands in order to develop S_u-V_{s1} relationships.

Results

Calculations were performed for each of the two sands, using three different values of K_o (0.4, 0.7 and 1.0) to capture the range of K_o values that will likely be encountered in practice. For each K_o condition for each sand, calculations were performed at 10 different values of σ_v' (from 5 kPa, to 200 kPa). At each stress level, the values of V_{s1} producing Ψ=0 represent the limiting value for contractant behaviour in a given sand.

Figure 3 presents the relationship between S_u/p' and state parameter for both sands. It can be seen that this is a unique relationship for a given sand and is independent of stress level or K_o. The curve for Ottawa sand is much steeper, due to the flatness of the SSL. Alaska sand, on the other hand, exhibits a more gradual decrease in shear strength ratio with increasing state parameter.

Figures 4(a) and (b) present plots of V_s versus σ_v' at a K_o of 0.4 for Ottawa sand and Alaska sand, respectively. Also shown on these plots are contours of V_{s1} and, hence, contours of S_u. These figures clearly indicate that the value of V_{s1} that acts as a dividing line between contractant and dilatant behaviour (i.e. $\Psi = 0$) is not constant with depth. Rather, the dividing value of V_{s1} increases with depth for either sand. These values, especially those for Ottawa sand, agree well with the suggested values of 140 m/s to 160 m/s by Robertson *et al* (1992a). The dividing value for Ottawa sand is closer to being a constant value with depth than Alaska sand due to the flatter SSL for Ottawa sand. Figure 4(a) or (b) could be used to evaluate field data in Ottawa or Alaska sand by superimposing a shear wave velocity profile over either plot in order to estimate the values

of S_u with depth. Note that, at a particular σ_v', S_u increases more gradually in Alaska sand than in Ottawa sand as V_s is increased.

Figure 5 presents a plot of S_u versus V_{s1} for both Ottawa and Alaska sand. It can be seen that for a given sand and a given K_o, S_u is a unique function of V_{s1}. As K_o increases, the S_u-V_{s1} line moves to the right as higher values of K_o will result in higher values of measured shear wave velocity. Comparing Ottawa sand to Alaska sand, it can be seen that the shapes and locations of the lines are quite different. This is due to the differences between the SSLs, reflected in λ_{in} and Γ. The S_u-V_{s1} relationship for Ottawa sand is sharper and divides more distinctly between sand with very little undrained strength and sand with high strength. The relationship for Alaska sand is more gradual, indicating a slower, steadier increase in strength as V_{s1} increases. Thus λ_{in}, Γ, and K_o are three major factors affecting the S_u-V_{s1} relationship.

Figure 6 compares the S_u-V_{s1} relationships for Ottawa and Alaska sand to the other sands tabulated by Sasitharan *et al* (1993), for K_o equal to 0.4. These figures illustrate that Ottawa and Alaska sand encompass most of the other sands on a plot of S_u versus V_{s1}. In addition, it is clear that most of the other sands have sharp S_u-V_{s1} relationships, similar to or sharper than that for Ottawa sand. Alaska sand has a more gradual relationship than any of the other sands. This is because most of the other sands plotted here have λ_{in} values similar to that for Ottawa sand whereas the value for Alaska sand is an order of magnitude greater. Comparing Leighton Buzzard and Ottawa sand, which have similar values of λ_{in} and ϕ'_{ss} (see Table 1), it can be seen that Leighton Buzzard sand, which has a higher value of Γ, plots to the left of Ottawa sand, although the lines for both sands have similar shapes. Therefore, the shape of the S_u-V_{s1} relationship appears to be controlled by λ_{in}, while Γ tends to control the position of the curve along the V_{s1}-axis. Thus, the relative shape and position of the S_u-V_{s1} relationships for the various sands parallels the relative slopes and positions of the SSL's in e-p' space for the various sands (see Figure 2a). The location of the SSL for a soil is given by the parameters Γ and λ_{in}. The slope of the SSL (λ_{in}) appears to be controlled

primarily by the compressibility of the soil. More compressible soils have steep SSL's (i.e. large values for λ_{1n}). The location of the SSL is controlled by Γ which appears to be influenced by the fabric of the soil, although further research is required to clarify this point.

Figure 7 illustrates the effect of adding fines to clean Ottawa sand on the relationship between S_u and V_{s1}, relative to clean Ottawa sand and Alaska sand for Ko equal to 0.4. Also included in Figures 7(a) and (b) is the relationship for kaolin. It can be seen that increasing the percent kaolinite from 0% to 10% moves the S_u-V_{s1} relationship to the right of the line for clean Ottawa sand. However, the relationship for kaolin (i.e. 100% kaolinite) plots to the left of the line for clean Ottawa sand, even further than the relationship for Alaska sand. As the percent kaolinite is increased from 0 to 10%, one would need to measure a higher V_{s1} to obtain the same S_u. However, if larger percentages of kaolinite were added (greater than 20%) the SSL moves upward to higher void ratios (Pitman 1993) and it would be reasonable to expect that the S_u-V_{s1} relationship would move back to the left and eventually, at 100% kaolinite, to approximately the location of the relationship for kaolin. This would be consistent with the observation made earlier that the S_u-V_{s1} plot parallels the SSL plot in e-p' space (see Figure 2b).

Conversion of V_{s1} to SPT $(N_1)_{60}$ and CPT q_{c1}

In order to compare the shear wave velocity method of estimating S_u, S_u/p' and S_u/σ_v' with the existing methods, V_{s1} must be converted to equivalent SPT $(N_1)_{60}$ and equivalent CPT q_{c1}. Yoshida *et al* (1988) proposed that shear wave velocity, V_s, and raw SPT N could be correlated using the following equation:

$$V_s = 94\, N^{0.25} \left(\frac{\sigma_v'}{P_a}\right)^{0.140} \quad \text{(m/s)} \qquad [25]$$

where:

$P_a = 100$ kPa

N = Japanese $N = \frac{N_{60}}{1.2}$ (blows per 30 cm) [26]

This equation is applicable to clean, unaged, uncemented, predominantly silica sands. In order to correlate $(N_1)_{60}$ with V_{s1}, equation 20, which relates V_{s1} to V_s, will be used in addition to the following equation relating $(N_1)_{60}$ to N:

$$(N_1)_{60} = N_{60} \left(\frac{P_a}{\sigma_v'}\right)^{0.5} = N \bullet \frac{ER}{60} \bullet \left(\frac{P_a}{\sigma_v'}\right)^{0.5} \quad [27]$$

where $P_a = 100$ kPa

However, when combined with the normalizations in equations 20 and 27, the correlation proposed by Yoshida *et al* (1988) does not give a unique correlation between $(N_1)_{60}$ and V_{s1}; rather, it gives a stress dependent correlation, as follows:

$$(N_1)_{60} = \left(\frac{V_{s1}}{89.8} \left(\frac{P_a}{\sigma_v'}\right)^{0.015}\right)^4 \quad [28]$$

V_{s1} and the equivalent $(N_1)_{60}$ should represent the same relative density and thus the correlation relating the two should not be stress level dependent. In order to eliminate the stress term from the above equation, the Yoshida *et al* (1988) correlation, given in equation 25, must be modified slightly, as follows:

$$V_s = 94\, N^{0.25} \left(\frac{\sigma_v'}{P_a}\right)^{0.125} \quad \text{(m/s)} \quad [29]$$

This slight modification is consistent with the database and reflects a minor correction to the stress exponent. When combined with the normalizations in equations 20 and 27, this results in the following equation to calculate the equivalent SPT $(N_1)_{60}$ from V_{s1}:

$$(N_1)_{60} = \left(\frac{V_{s1}}{89.8}\right)^4 \qquad [30]$$

where V_{s1} is in units of m/s

Robertson *et al* (1992b) proposed that shear wave velocity, V_s, and CPT tip resistance, q_c, could be correlated using the following equation, similar to that relating V_s and N, as proposed by Yoshida *et al* (1988):

$$V_s = 102\, q_c^{0.23} \left(\frac{\sigma_v'}{P_a}\right)^{0.135} \quad \text{(m/s)} \qquad [31]$$

where q_c is in units of MPa

In order to correlate q_{c1} with V_{s1}, equation 20, which relates V_{s1} to V_s, will be used in addition to the following equation relating q_{c1} to q_c:

$$q_{c1} = q_c \left(\frac{P_a}{\sigma_v'}\right)^{0.5} \qquad [32]$$

where $P_a = 100$ kPa

This results in the following equation to calculate the equivalent CPT q_{c1} from V_{s1}:

$$q_{c1} = \left(\frac{V_{s1}}{102}\right)^{4.35} \quad \text{(MPa)} \qquad [33]$$

where Vs1 is in units of m/s

Notice that, as for equation 30, stress level does not come into the relationship. Equations 30 and 33 can be combined with equation 22 to produce equations for estimating S_u from $(N_1)_{60}$ and q_{c1} in clean, unaged, uncemented, predominantly silica sands, as follows:

$$S_u = \frac{M}{2}\exp\left[\frac{1}{\lambda_{1n}}\left(\frac{89.8\,(N_1)_{60}^{0.25}}{B\,(K_o)^{na}} - \left(\frac{A}{B} - \Gamma\right)\right)\right] \qquad \text{(kPa)} \qquad [34]$$

where λ_{1n} has units of $\frac{1}{ln(\text{kPa})}$

and:

$$S_u = \frac{M}{2}\exp\left[\frac{1}{\lambda_{1n}}\left(\frac{102\,q_{c1}^{0.23}}{B\,(K_o)^{na}} - \left(\frac{A}{B} - \Gamma\right)\right)\right] \qquad \text{(kPa)} \qquad [35]$$

where q_{c1} is in MPa and λ_{1n} has units of $\frac{1}{ln(\text{kPa})}$

For a given sand, equations 22, 34 and 35 for S_u are not solely functions of V_{s1}, $(N_1)_{60}$ or q_{c1}, respectively; they are also dependent on K_o. However, examining these three equations, it can be seen that, for na=nb=0.125, they are unique functions of $V_{s1}/(K_o)^{0.125}$, $(N_1)_{60}/(K_o)^{0.5}$, and $q_{c1}/(K_o)^{0.543}$, respectively. Plotting S_u versus $V_{s1}/(K_o)^{0.125}$, $(N_1)_{60}/(K_o)^{0.5}$, or $q_{c1}/(K_o)^{0.543}$ would result in a single relationship equivalent to S_u versus V_{s1}, $(N_1)_{60}$, or q_{c1}, respectively, for a K_o of 1.0.

Equations 30 and 33 can be combined with equation 23 to produce equations for estimating S_u/p' from $(N_1)_{60}$ and q_{c1} in clean, unaged, uncemented, predominantly silica sands, as follows:

$$\frac{S_u}{p'} = \frac{M}{2}\,\frac{\exp\left[\frac{89.8\,(N_1)_{60}^{0.25}}{B\,(K_o)^{0.125}} - \lambda_{1n}\,ln\left(\frac{\sigma_v'}{3}(1+2Ko)\right)\right]}{\exp\left(\frac{A}{B} - \Gamma\right)} \qquad [36]$$

and:

$$\frac{S_u}{p'} = \frac{M}{2}\,\frac{\exp\left[\frac{102\,q_{c1}^{0.23}}{B\,(K_o)^{0.125}} - \lambda_{1n}\,ln\left(\frac{\sigma_v'}{3}(1+2Ko)\right)\right]}{\exp\left(\frac{A}{B} - \Gamma\right)} \qquad [37]$$

The effect of compressibility on V_{s1}-$(N_1)_{60}$ and V_{s1}-q_{c1} correlations

Compressibility will not affect the measured shear wave velocity since shear waves do not compress the sand, but it can greatly affect the SPT and CPT penetration resistance since the more compressible the sand is, the lower the penetration resistance, even at the same relative density (Robertson and Campanella 1983). Therefore, it follows that there cannot be a unique correlation between V_s and N or between V_s and q_c for all sands, due to differences in compressibility between sands. Equations 30 and 33 were developed based on the work by Yoshida *et al* (1988) and Robertson *et al* (1992b). Both of these proposals were developed using relatively incompressible clean, unaged, uncemented, predominantly silica sands. Thus equations 30 and 33 should be reasonably applicable to Ottawa sand which is also relatively incompressible and is a clean quartz sand. However, Alaska sand is a very compressible sand and therefore, equations 30 and 33 are not applicable.

Shear wave velocity, SPT and CPT profiles were available from the tailings sand site in Alaska. Examining these profiles, the relationships between V_s and N and V_s and q_c in Alaska sand were determined to be as follows:

$$V_s = 113\ N^{0.25}\ \left(\frac{\sigma_v'}{P_a}\right)^{0.125} \qquad [38]$$

$$V_s = 135\ q_c^{0.23}\ \left(\frac{\sigma_v'}{P_a}\right)^{0.135} \qquad [39]$$

Assuming $N=N_{60}$ at the Alaska site, this results in the following equations relating $(N_1)_{60}$ to V_{s1} and q_{c1} to V_{s1} in Alaska sand:

$$(N_1)_{60} = \left(\frac{V_{s1}}{113}\right)^4 \qquad [40]$$

$$q_{c1} = \left(\frac{V_{s1}}{135}\right)^{4.35} \qquad [41]$$

Comparing equations 30 and 33 for incompressible sand and equations 40 and 41 for compressible Alaska sand, one can see that equations 40 and 41 will give lower values of penetration resistance for the same value of V_{s1}. Note also that the constants in these equations reflect the compressibility of the sand. In the field, lower SPT blowcounts or CPT q_c would be measured in Alaska sand than would be predicted based on shear wave velocity measurements and the conversion equations for incompressible sands. Thus, for Alaska sand, the equations relating S_u and S_u/p' to $(N_1)_{60}$ would be the same as equations 34 and 36, respectively, except that the constant 89.8 for Ottawa sand would be replaced by the constant 113 for Alaska sand. Similarly, the equations relating S_u and S_u/p' to q_{c1} would be the same as equations 35 and 37, respectively, except that the constant 102 for Ottawa sand would be replaced by the constant 135 for Alaska sand.

Sensitivity of the proposed method to the input parameters

The discussion presented thus far revolves around the assumption that K_o and the soil parameters ϕ'_{ss}, Γ, λ_{1n}, A and B can be determined with certainty. However, in reality, although each parameter will have a "best-fit" value, it will also have a possible range of values that it may possess due to the uncertainty associated with estimating its true value.

It is evident from Figure 5 that K_o plays a major role in the relationship between S_u and shear wave velocity. However, K_o is often a very difficult parameter to determine in the field. Clearly, having a good estimate of the value of K_o or at least the range in which it may fall in the field will allow for a better estimate of S_u. K_o has a direct impact on S_u since the values of V_{s1}, $(N_1)_{60}$ and q_{c1} measured in the field are proportionate to the value of K_o.

Determining the steady state friction angle, ϕ'_{ss}, using stress-strain curves from conventional triaxial tests is straightforward and should have good accuracy (± 1°) for a particular sand. In addition, ϕ'_{ss} only affects the parameter M in the equation for S_u and, thus, S_u should be relatively insensitive to small changes in ϕ'_{ss}.

Γ and λ_{ln} define the location of the SSL in e-*ln* p' space. A sand with a higher value of λ_{ln} is generally more compressible. A sand with a higher value of Γ has its SSL at higher void ratios and therefore has a steady state condition defined by a looser state for a given λ_{ln} and a given level of stress. For a particular sand, these parameters are determined from the best-fit line to a series of data points at steady state. Therefore, there will be a certain degree of scatter to the data and there will be some uncertainty associated with both parameters. This uncertainty can be minimized by careful laboratory testing procedures.

The parameters A and B define the relationship between V_{s1} and void ratio. For a particular sand, these parameters are determined for the best-fit line to a series of data points in V_{s1}-e space during consolidation. Therefore, as for Γ and λ_{ln}, there will be a certain degree of scatter to the data and there will be some uncertainty associated with both A and B (see Table 1). This uncertainty can also be minimized by careful laboratory procedures.

All of the graphs presented thus far have only shown the results based on the "best-fit" values of ϕ'_{ss}, Γ, λ_{ln}, A and B for the two particular sands. However, the possible degrees of inaccuracy associated with these parameters will translate into zones rather than unique lines on the various plots relating S_u to shear wave velocity and penetration resistances. Figures 8 shows the zones of uncertainty on the plot of S_u versus V_{s1} resulting from the possible ranges for the individual values of A and B for Ottawa sand and Alaska sand for K_o equal to 0.4. It can be seen that the zone of inaccuracy is smaller for Alaska sand than for Ottawa sand. This is partly due to the fact that Alaska sand has a steeper SSL which is less sensitive to small changes in void ratio and partly due

to the fact that B has a smaller range of uncertainty for Alaska sand than for Ottawa sand. For Ottawa sand, the band of uncertainty is sufficiently wide that S_u cannot be estimated accurately. The best that can be achieved for Ottawa sand is to determine whether the field profiles fall below or above this band in order to determine whether or not undrained stability will be an issue. These zones on plots relating S_u to shear wave velocity cannot be directly translated into zones on the corresponding plots for the SPT and CPT methods; there may be other factors contributing to such zones of uncertainty due to the nature of the SPT and CPT.

Ultimate steady state versus quasi steady state

This study has considered the ultimate undrained steady state shear strength of sand determined from triaxial compression loading and shown how to estimate its magnitude from the ultimate SSL using shear wave velocity. The ultimate SSL and S_u are independent of initial fabric since the soil is remoulded by the time steady state is reached. Some argue that the quasi steady state (QSS) strength is more critical for stability analyses than the steady state strength (Ishihara 1993). Whether or not this is true will not be discussed in great detail here. However, it is possible that QSS may be a feature of the type of loading. In addition, even if such a QSS does exist, if a slope started to slide due to the lower QSS strength in a particular region, the additional straining may quickly bring this material up to the ultimate-steady state strength at large strains. Thus, S_u would ultimately control the stability of such a slope, although there may be some inertial effects due to the initial movement that would have to be considered.

Some research has also suggested that the SSL and hence S_u is significantly smaller in triaxial extension than triaxial compression (Vaid 1990; Negussey 1994). Nevertheless, if one were interested in QSS or S_u in extensional loading, the same procedure could be used to estimate the undrained strength, given that the parameters Γ, λ_{1n}, and ϕ'_{ss} are determined for either the quasi steady state line (QSSL) or the SSL for extensional loading. Since both the QSSL and extensional

loading can produce lower values of S_u, the resulting correlations between V_{s1} and S_u will produce lower values of undrained shear strength than those suggested here.

COMPARISON OF THE EQUIVALENT SPT AND CPT PLOTS WITH THE CURRENT METHODS OF ESTIMATING S_u

Figure 9 presents the results of S_u versus equivalent $(N_1)_{60}$ determined using the results of Figure 5 together with equation 30 for clean Ottawa sand and equations 30 (the incompressible correlation, referred to as Alaska (I)) and 40 (accounting for compressibility, referred to as Alaska (C)) for Alaska sand. The other sands tabulated by Sasitharan *et al* (1993) and Ottawa sand with the various percentages of kaolinite cannot be included here since no data are available to allow for a conversion from V_{s1} to $(N_1)_{60}$ in such materials. However, it would seem reasonable to hypothesize that the S_u-$(N_1)_{60}$ lines for Ottawa sand plus kaolinite would plot to the left of clean Ottawa sand since one would expect to record lower blowcounts in a material with a higher fines content.

Results from the investigation into the stability of Duncan Dam are also shown in Figure 9 (BC Hydro, 1993). The site investigation results for Duncan Dam indicated an increase in $(N_1)_{60}$ with increasing vertical effective stress in the sand zone in which liquefaction was predicted to be triggered by the design earthquake. Lab testing of frozen undisturbed samples of this sand indicated that a constant ratio of S_u/σ_v' of 0.21 could be used to estimate S_u with depth. Combining the field and lab results allowed for the relationship between S_u and (N1)60 to be plotted as shown in Figure 9. The relationship for Duncan Dam is clearly similar to the results of this study, having a similar shape and location on the plot and, in particular, showing S_u to increase with increasing $(N_1)_{60}$ at a similar rate to the relationships for Ottawa sand and Alaska sand.

Superimposed on Figure 9, for purpose of comparison, are the upper and lower bound lines relating S_u to $(N_1)_{60}$ from Seed and Harder (1990). It can be seen that there is a relationship between S_u and $(N_1)_{60}$, as Seed and Harder were suggesting. However, this relationship is unique only for a given sand and a given K_o-condition. This study has shown that K_o plays an important role in the S_u-$(N_1)_{60}$ relationship for any given sand and that the differences in compressibility and fabric between Ottawa sand and Alaska sand result in very different relationships between S_u and $(N_1)_{60}$. The empirical plot by Seed and Harder (1990) incorporates 17 case histories involving different types of sand and likely involving different conditions of K_o. Hence, the framework presented in this study can account for the scatter in the Seed and Harder (1990) plot by attributing it in part to variations in compressibility, fabric and K_o amongst the various case histories. Alaska sand to Ottawa sand should encompass most types of sands that will be encountered in practice and yet, the Seed and Harder (1990) lines appear much flatter, predicting much lower strengths at the same $(N_1)_{60}$, even for Ottawa sand, at higher values of $(N_1)_{60}$. The Seed and Harder (1990) lines are also much flatter than the results for Duncan Dam. It is possible that other factors which have not been taken into account here, such as pore pressure redistribution, may be responsible for the differences between the Seed and Harder (1990) lines derived from case histories and the results of this study.

The plot by Seed and Harder (1990) is for the equivalent SPT $(N_1)_{60}$ in clean sand. Thus, for the case histories in sand with fines, a fines content correction was applied to increase the value of the measured $(N_1)_{60}$ to reflect what the equivalent $(N_1)_{60}$ would be in clean sand. The fines content corrections (ΔN_1) suggested by Seed (1987) are as follows: $\Delta N_1 = 1, 2, 4$ and 5 for fines contents of 10%, 25%, 50% and 75%, respectively. Seed (1987) explained that these were tentative values, but that judgement should be exercised in applying the corrections due to differences between different soils. Although not explained as such by Seed (1987), it is felt by the authors that these correction factors were an attempt to account for the increased compressibility of sand with fines relative to clean sand. Looking at the results of this study for Alaska sand which has a

fines content of about 31%, it can be seen that the difference between the Alaska (I) results and the Alaska (C) results varies with $(N_1)_{60}$ and K_o, but has an average $\Delta(N_1)_{60}$ of approximately 3. This is consistent with the correction factors suggested by Seed (1987).

Note that, although fines content may be an indirect measure of compressibility, clean sands may also be compressible. For these sands, such as clean carbonate sands, Seed (1987) would not recommend a correction factor, whereas the method followed here would directly incorporate the compressibility of the sand into the relationship between S_u and $(N_1)_{60}$. A sand with high shear wave velocities and high penetration resistances represents a dense, incompressible sand; a sand with low shear wave velocities and low penetration resistances represents a loose sand. However, a sand with high shear wave velocities, but low penetration resistances likely represents a stiff, but compressible sand. This latter type of sand could be much stronger than one would initially expect, based on penetration resistance. Alaska sand is a good example of such a sand.

Figure 10 presents the results of S_u/σ_v' versus equivalent $(N_1)_{60}$ determined by combining equation 24 with equation 30 for clean Ottawa sand and with equations 30 (the incompressible correlation, referred to as Alaska (I)) and 40 (accounting for compressibility, referred to as Alaska (C)) for Alaska sand. For the reasons explained above, the other sands from Sasitharan *et al* (1993) and Ottawa sand plus kaolinite are not included on this figure. Superimposed on Figure 10, for purpose of comparison, are the upper bound, lower bound and average lines relating S_u/σ_v' to $(N_1)_{60}$ from Stark and Mesri (1992). It can be seen that, contrary to the suggestion by Stark and Mesri, there is no unique relationship between S_u/σ_v' and $(N_1)_{60}$. Although the 20 case histories in Stark and Mesri's plot appear to follow a trend, there is a lot of scatter. This is likely due to differences in compressibility, fabric and K_o between case histories, as in the Seed and Harder plot, but is also compounded by the fact that S_u/σ_v' and $(N_1)_{60}$ are not related by a unique relationship, even for a given sand and K_o-condition. Two case histories involving similar types of sands and K_o-conditions, would not plot in the same place on the plot if the stress levels were

different. As for the Seed and Harder (1990) plot, Stark and Mesri's (1992) plot is for the equivalent $(N_1)_{60}$ in clean sand. The same comments, outlined above, regarding the relationship between compressibility and fines content apply here.

Figure 11 presents the results of S_u versus equivalent q_{c1} using the results of Figure 5 and equation 33 for clean Ottawa sand and equation 41 for Alaska sand. The other sands from Sasitharan *et al* (1993) and Ottawa sand with the various percentages of kaolinite cannot be included here since no data are available to allow for conversions from V_{s1} to q_{c1} in such materials. However, it would seem reasonable to hypothesize that the S_u-q_{c1} lines for Ottawa sand plus kaolinite would plot to the left of clean Ottawa sand since one would expect to record lower cone tip resistances in a material with a higher fines content. Superimposed on Figure 11 are the results from Robertson (1990). This figure illustrates that Ottawa sand and Alaska sand encompass several other types of sands, with the exception of Monterey sand, and therefore likely represent two extremes of the types of sands that could be encountered in practice. Ottawa sand and Alaska sand both show that there is a unique relationship between S_u and q_{c1} for a given Ko, agreeing with the work by Robertson (1990). The lines for Ottawa sand from this study and from that by Robertson (1990) are both lower bounds for the given sands; however, there is some difference. The line for Alaska sand falls in the range of other compressible sands such as Hilton Mines tailings. Robertson (1990) suggested that the relationships were approximate in nature due to the limited test data and the complex series of assumptions required.

Figure 12 presents S_u/p' versus normalized CPT penetration resistance, $(q_c-p)/p'$ for both Ottawa sand and Alaska sand calculated for K_o=0.5, since Robertson's (1990) results which are superimposed on this figure were for a K_o of 0.5. Assumptions made in calculating p from p' in order to produce this figure included a groundwater table located at a depth of 1.0 m and a unit weight for both Ottawa and Alaska sand of 18 kN/m^3. Again, it can be seen that, in general, Ottawa sand and Alaska sand encompass several other types of sands and therefore represent two

extremes of the types of sands that will be encountered in practice. However, Figure 12 also shows that there is not a unique relationship between S_u/p' and normalized q_{c1} as was suggested by Jefferies et al. (1990). Rather, a series of lines are produced which are stress level dependent. Robertson's (1990) unique lines for each sand are based on the proposal by Been and Jefferies (1987) that there is a unique relationship between state parameter and normalized CPT penetration resistance. The fact that the results of this study indicate a dependency on stress by the relationship between S_u/p' and normalized CPT suggests that the relationship between state parameter and normalized CPT resistance is not unique. This agrees with the comments made by Sladen (1989) upon revisiting the data obtained in CPT calibration chamber testing by Been and Jefferies (1987); i.e. "the relationship is not unique for all stress levels - rather, it varies systematically with mean stress level".

CONCLUSIONS

This study has combined critical state soil mechanics and shear wave velocity measurements in order to develop a framework which can be used to estimate the *in-situ* ultimate undrained steady state shear strength of a sand. In the process, the range of values that can be expected to encompass most sands on plots of S_u versus V_{s1}, q_{c1} or $(N_1)_{60}$ has been shown and has been attributed primarily to the location of the SSL in terms of Γ and λ_{1n} as well as K_o. More compressible sands tend to have larger values of λ_{1n}. The plot of S_u versus $(N_1)_{60}$ by Seed and Harder (1990) appears conservative, especially for compressible sands with high values of λ_{1n} and Γ and for site conditions producing low values of K_o.

This study has also demonstrated that it is unlikely to have a unique relationship between S_u/σ_v' and $(N_1)_{60}$, as suggested by Stark and Mesri (1992) or between S_u/p' and normalized CPT resistance, as suggested by Been and Jefferies (1990). The empirical case histories do suggest such a relationship, in that the general trend is an increase in S_u/σ_v' or S_u/p' as $(N_1)_{60}$ or

normalized CPT resistance increases. However, encompassed in the empirical case histories or the results of calibration chamber testing is the fact that the relationships are stress level dependent for a given sand, in addition to being dependent on compressibility and differences in K_o between sands. A constant S_u/p' or S_u/σ_v' ratio can only be used on a site-specific basis when Ψ is a constant.

Finally, the application of the proposed method relies on laboratory work to determine the parameters of the SSL (ϕ'_{ss}, Γ, λ_{ln}) and the parameters relating V_{s1} to e for a particular sand (A and B). Although the method appears quite promising, it is not without drawbacks. The level of accuracy in estimating S_u using shear-wave velocity may present some problems and should be considered when applying the method. If the SSL of a sand is relatively flat ($\lambda_{ln} < 0.035$), it will not be possible to accurately determine S_u using shear wave velocity measurements or *in-situ* penetration testing. Note that this is the case for most of the uniform, clean silica sands included in this paper. However, for such sands, it will be possible to determine the dividing line, in terms of V_{s1}, $(N_1)_{60}$, or q_{c1}, between soil conditions that will exhibit essentially little or no strength when loaded undrained and soil conditions that will be able to fully mobilize the steady state drained friction angle. A further complication when estimating S_u from *in-situ* tests is the possible effects of pore pressure redistribution after cyclic (earthquake) loading.

ACKNOWLEDGEMENTS

The authors would like to thank S. Sasitharan, J. Cunning and R. Skirrow for their time and effort spent determining the soil parameters in the laboratory. Steffen, Robertson and Kirsten (Canada) Inc. kindly provided the field data for Alaska sand. C. Fear would like to gratefully acknowledge the Natural Sciences and Engineering Research Council of Canada for her 1967 NSERC Science and Engineering Scholarship and the Alberta Heritage Trust Fund for her Ralph Steinhauer Award of Distinction.

NOTATION

A	= intercept of V_{s1}-axis at e=1.0 on a V_{s1}-e plot, in m/s
B	= slope of V_{s1}-e plot, in m/s
C	= A/B - Γ
C_N	= SPT overburden correction factor = $(P_a/\sigma_v')^{0.5}$
CPT	= Cone Penetration Test
D_r	= relative density
e	= void ratio
ER	= Energy Ratio of SPT, in %
e_{ss}	= void ratio at steady state
K_o	= ratio of horizontal stress to vertical stress
M	= ratio of q to p' along the SSL = q_{ss}/p'_{ss}
na	= stress exponent, typically = 0.125
nb	= stress exponent, typically = 0.125
N	= raw SPT blowcounts
N_{60}	= N • ER/60
$(N_1)_{60}$	= C_N • N_{60}
P_a	= atmospheric or reference pressure; generally taken to be 100 kPa
p'	= mean normal effective stress = 1/3 (σ_1' + 2 σ_3')
p_o'	= initial mean normal effective stress
p_{ss}'	= mean normal effective stress at steady state
q	= deviator stress = σ_1' - σ_3'
q_{ss}	= deviator stress at steady state
q_c	= raw CPT cone tip resistance
q_{c1}	= CPT cone tip resistance, corrected to σ_v' = 100 kPa
QSS	= Quasi Steady State
QSSL	= Quasi Steady State Line

SPT = Standard Penetration Test

SSL = Steady State Line

S_u = ultimate undrained steady state shear strength of sand

S_{uq} = QSS undrained shear strength of sand

V_s = raw shear-wave velocity

$V_{s\Psi}$ $= \dfrac{V_s\,(P_a)^{0.25}}{B\,(\sigma_a')^{0.125}\,(\sigma_p')^{0.125}} - \lambda_{1n}\,ln\,p'$

V_{s1} = shear-wave velocity, corrected to $\sigma_v' = 100$ kPa

ΔN_1 = fines content correction proposed by Seed (1987)

Γ = intercept of the SSL in e-*ln* p' or e-log p' space at p'=1.0 kPa

λ = slope of the SSL

λ_{1n} = slope of the SSL in e-*ln* p' space

λ_{1og} = slope of the SSL in e-log p' space

ϕ'_{ss} = steady state drained friction angle

σ_1' = major principal effective stress

σ_3' = minor principal effective stress

σ_a' = effective stress in the direction of wave propagation, in kPa

σ_v' = vertical effective stress

σ_h' = horizontal effective stress

σ_p' = effective stress in the direction of particle motion, in kPa

Ψ = state parameter = e - ess

REFERENCES

Atkinson, J. 1993. An introduction to the mechanics of soils and foundations, McGraw-Hill, London, pp. 103-123.

B.C. Hydro. 1993. Duncan Dam liquefaction assessment and seismic stability, Report No. H2599, Hydroelectric Engineering Division, Geotechnical Department.

Been, K., Crooks, J.H.A., Becker, D.E., and Jefferies, M.G. 1986. The cone penetration test in sands: part I, state parameter interpretation. Geotechnique, **36**(2): 239-249.

Been, K., Jefferies, M.G., Crooks J.H.A., and Rothenburg, L. 1987. The cone penetration test in sands: part II, general inference of state. Geotechnique, **37**(3): 285-299.

Been, K., and Jefferies, M.G. 1985. A state parameter for sands. Geotechnique, **35**(2): 99-112.

Cunning J.C. 1994. Shear wave velocity measurement of cohesionless soils for evaluation of in-situ state, M.Sc. Thesis, Department of Civil Engineering, University of Alberta at Edmonton, Alberta.

Ishihara, K. 1993. Liquefaction and flow failure during earthquakes. The 33rd Rankine Lecture, London, England.

Jefferies, M.G., Been, K., and Hachey, J.E. 1990. Influence of scale on the constitutive behaviour of sand. Proceedings of the Canadian Geotechnical Engineering Conference, Laval University, **1**: 263-273.

Pitman, T.D. 1993. Effect of fines and gradation of the collapse surface of a loose saturated soil, Masters thesis, Department of Civil Engineering, University of Alberta at Edmonton, Alberta.

Robertson, P.K. 1990. Evaluation of residual shear strength of sands during liquefaction from penetration tests. Proceedings of the Canadian Geotechnical Engineering Conference, Laval University, **1**: 257-262.

Robertson, P.K., and Campanella, R.G. 1983. Interpretation of cone penetration tests. Part I: Sand. Canadian Geotechnical Journal, **20**(4): 718-733.

Robertson, P.K., Sasitharan, S., Cunning, J.C., and Sego, D.C. 1994. Shear wave velocity to evaluate flow liquefaction. Submitted to the Journal of Geotechnical Engineering: ASCE.

Robertson, P.K., Woeller, D.J., and Finn, W.D.L. 1992. Seismic cone penetration test for evaluation liquefaction potential under cyclic loading. Canadian Geotechnical Journal, **29**: 686-695.

Robertson, P.K., Woeller, D.J., Kokan, M., Hunter, J., and Luternauer, J. 1992. Seismic techniques to evaluate liquefaction potential. 45th Canadian Geotechnical Conference: 5:1-5:7.

Sasitharan, S. 1994. Collapse behaviour of very loose sand, Ph.D. Thesis, Department of Civil Engineering, University of Alberta at Edmonton, Alberta.

Sasitharan, S., Robertson, P.K., Sego, D.C., and Morgenstern, N.R. 1993. State boundary surface for very loose sand and its practical implications. Submitted to the Canadian Geotechnical Journal

Seed, H.B. 1987. Design problems in soil liquefaction. Journal of Geotechnical Engineering, **113**(8): 827-845.

Seed, R.B., and Harder, L.F. 1990. SPT-based analysis of cyclic pore pressure generation and undrained residual strength. Proceedings of the H. Bolton Seed Memorial Symposium, **2**: 351-376.

Skirrow, R. 1994. M.Sc. Thesis (in progress), Department of Civil Engineering, University of Alberta at Edmonton, Alberta.

Sladen, J.A. 1989. Problems with interpretation of sand state from cone penetration test. Canadian Geotechnical Journal, **39**: 323-332.

Sladen, J.A., D'Hollander, R.D., and Krahn, J. 1985. The liquefaction of sands, a collapse surface approach. Canadian Geotechnical Journal, **24**: 564-578.

Stark, T.D., and Mesri, G. 1991. Undrained shear strength of liquefied sands for stability analysis. Journal of Geotechnical Engineering, ASCE **118**(11): 1727-1747.

Vaid, Y.P., Chung, E.K.F., and Kuerbis, R.H. 1990. Stress path and steady state. Canadian Geotechnical Journal, **27**: 1-7.

Wood, D.M. 1990. Soil Behaviour and Critical State Soil Mechanics. Cambridge University Press, pp. 179-188.

Yoshida, Y., Ikemi, M., and Kokusho, T. 1988. Empirical formulas of SPT blow-counts for gravely soils. Proceedings of Penetration Testing, Balkema, Rotterdam, **1**: 381-387.

TABLES

FIGURES

TABLE 1. Material properties for (a) Ottawa sand and Alaska sand (Cunning 1994) (b) other sands (Sasitharan *et al* 1993).

(a)

	ϕ'_{ss}	Γ	λ_{1n}	A	B
Ottawa	30.5	0.926	0.0324	385.5*	261.8
Alaska	36.5	1.485	0.1172	319.5**	178.7
Ottawa+5% fines	29.5	0.809	0.029	***	***
Ottawa+7.5% fines	29.6	0.835	0.052	***	***
Ottawa+10% fines	29.4	0.930	0.103	***	***
Kaolin #	25	1.92	0.181	***	***

(b)

	ϕ'_{ss}	Γ	λ_{1n}	A	B
Erksak	30.9	0.82	0.0133	***	***
Toyoura (p'ss<100 kPa)	30.9	0.938	0.0043	***	***
Toyoura (p'ss=100 to 1000 kPa)	30.9	1.048	0.0283	***	***
Lornex	35	1.1	0.022	***	***
Brenda	35.9	1.112	0.042	***	***
Syncrude	29.8	0.847	0.017	***	***
Nerlerk	30	0.885	0.0145	***	***
Leighton Buzzard	29.8	1	0.0347	***	***

Notes:

* range = 371 to 397 m/s

** range = 314 to 326 m/s

*** use global values of A = 363 m/s (range = 340 to 380 m/s) and B = 235 m/s

\# ϕ'_{ss} cited by Atkinson (1993); λ_{1n} & Γ based on PI=32%, Gs=2.70, and formulae in Atkinson (1993)

TABLE 1

(a)

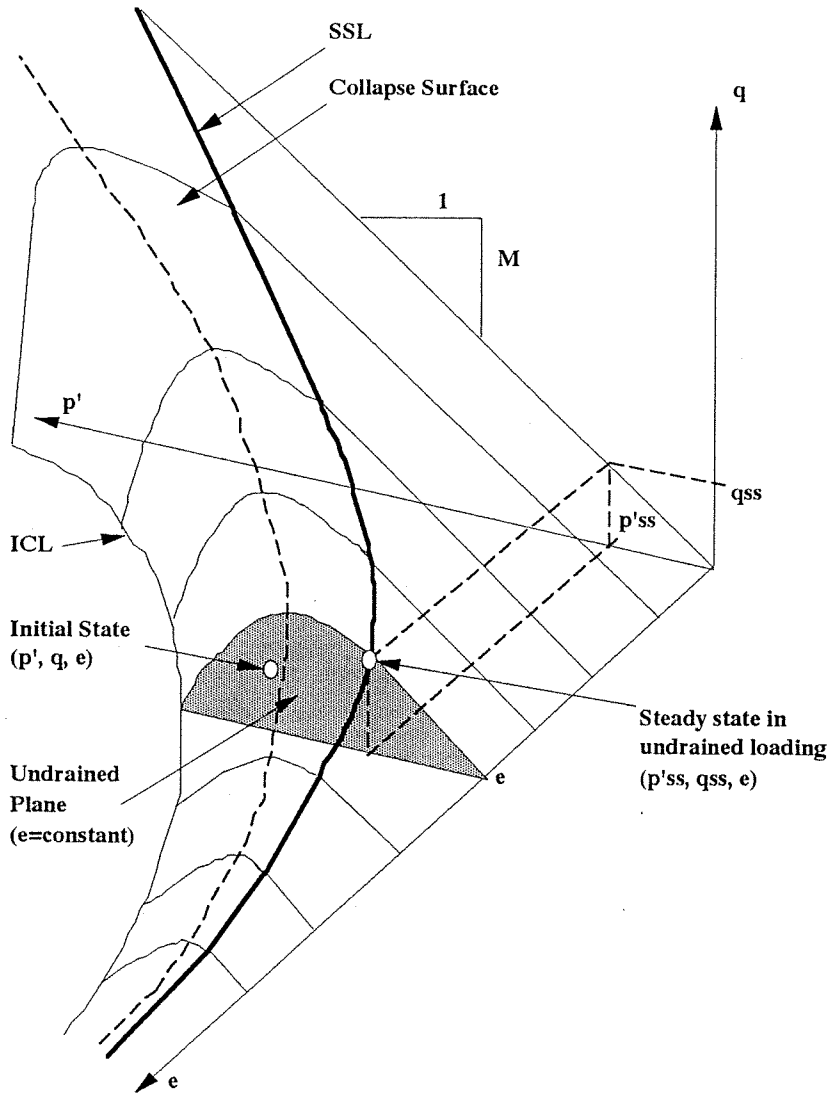

(b)

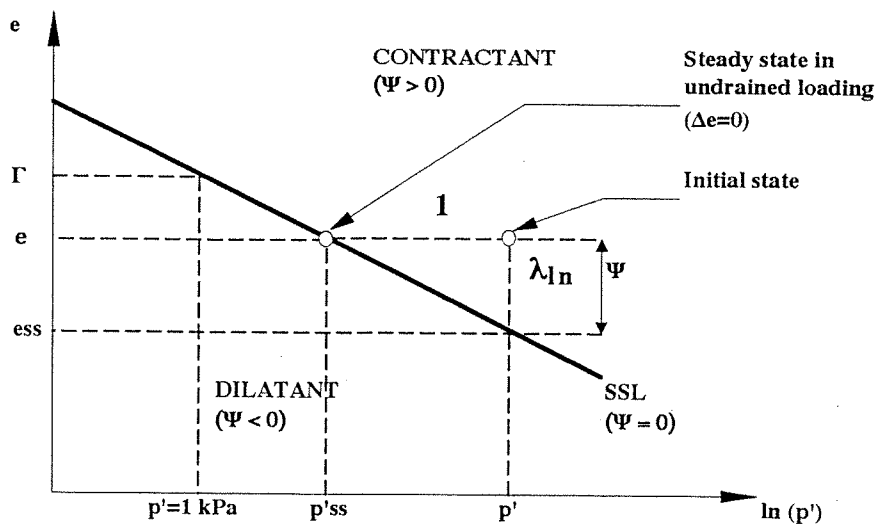

FIGURE 1(a)+(b)

(a)

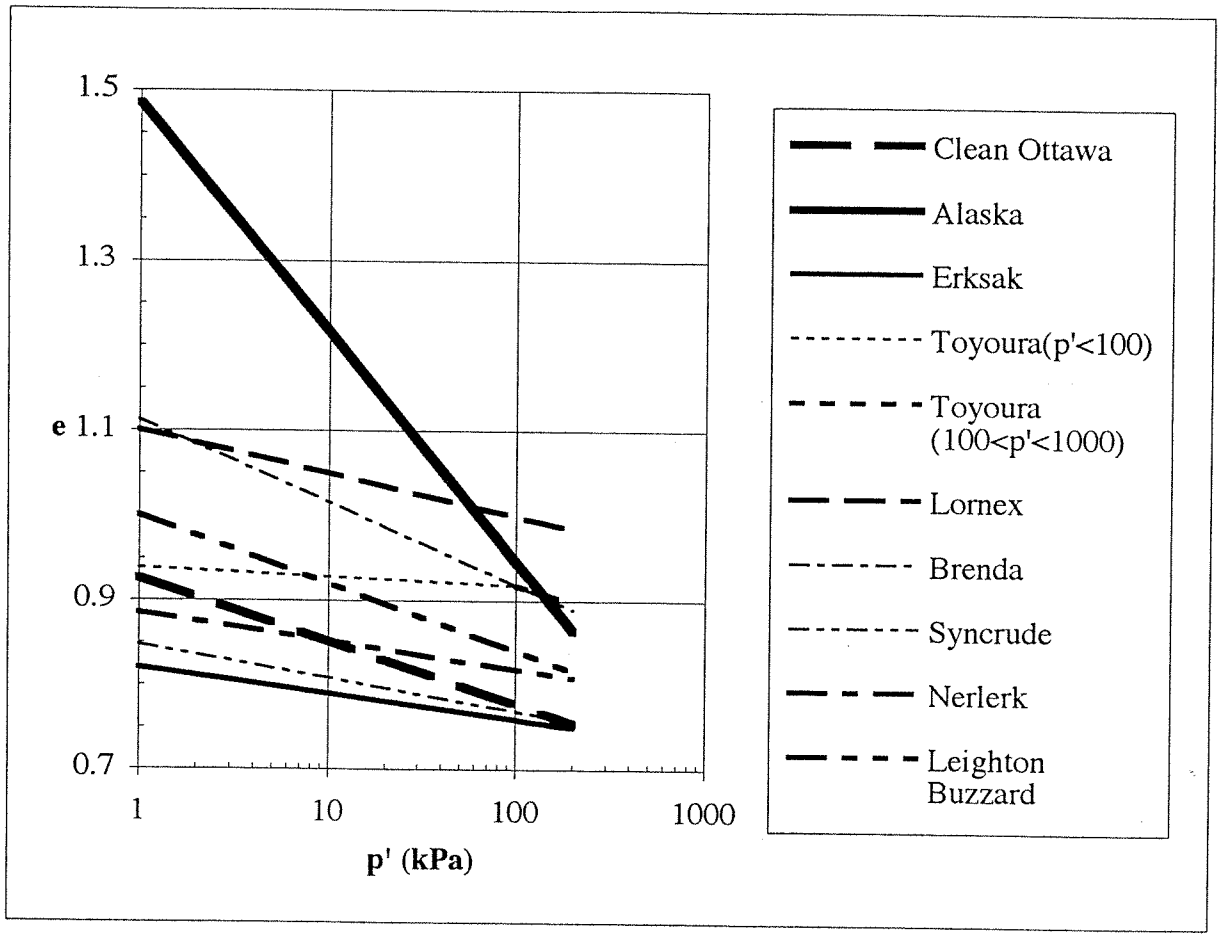

(b)

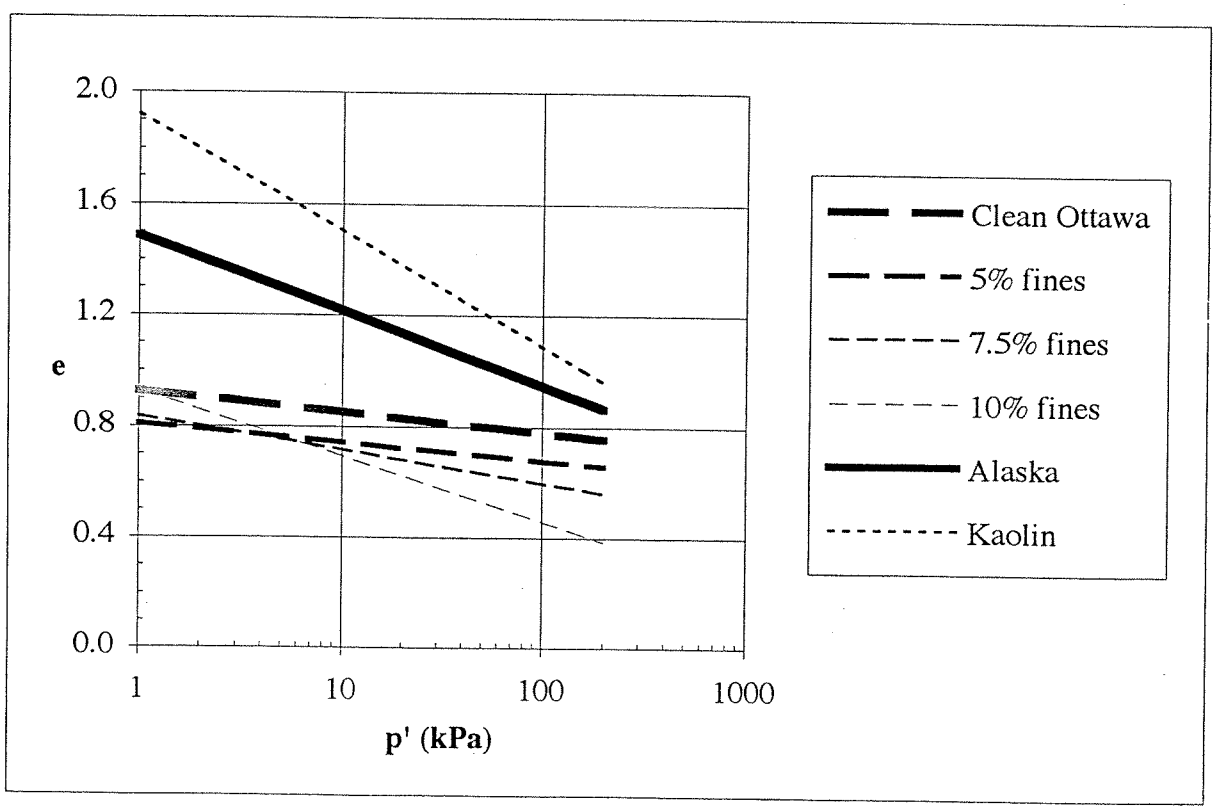

FIGURE 2(a)+(b)

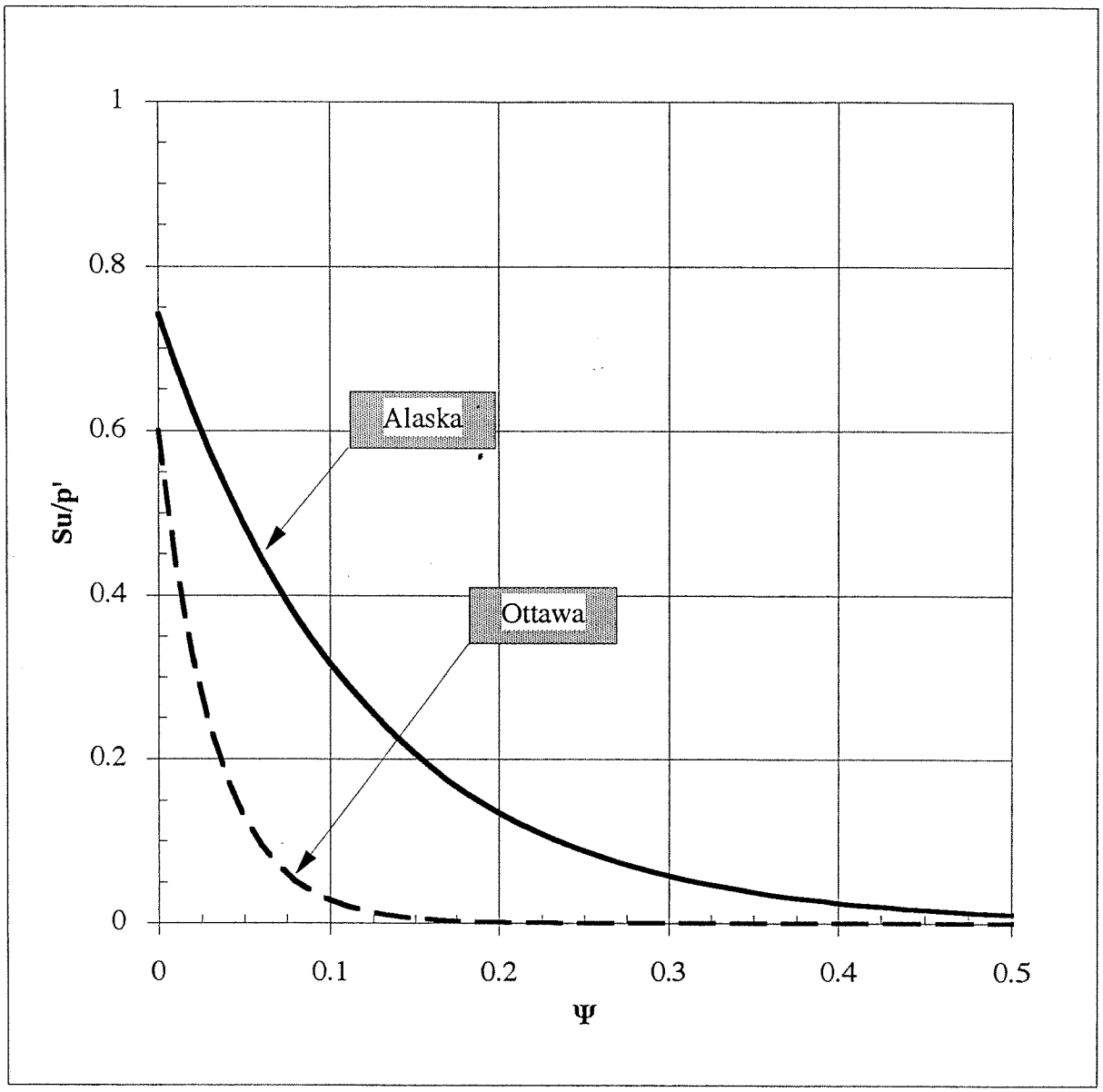

FIGURE 3

(a)

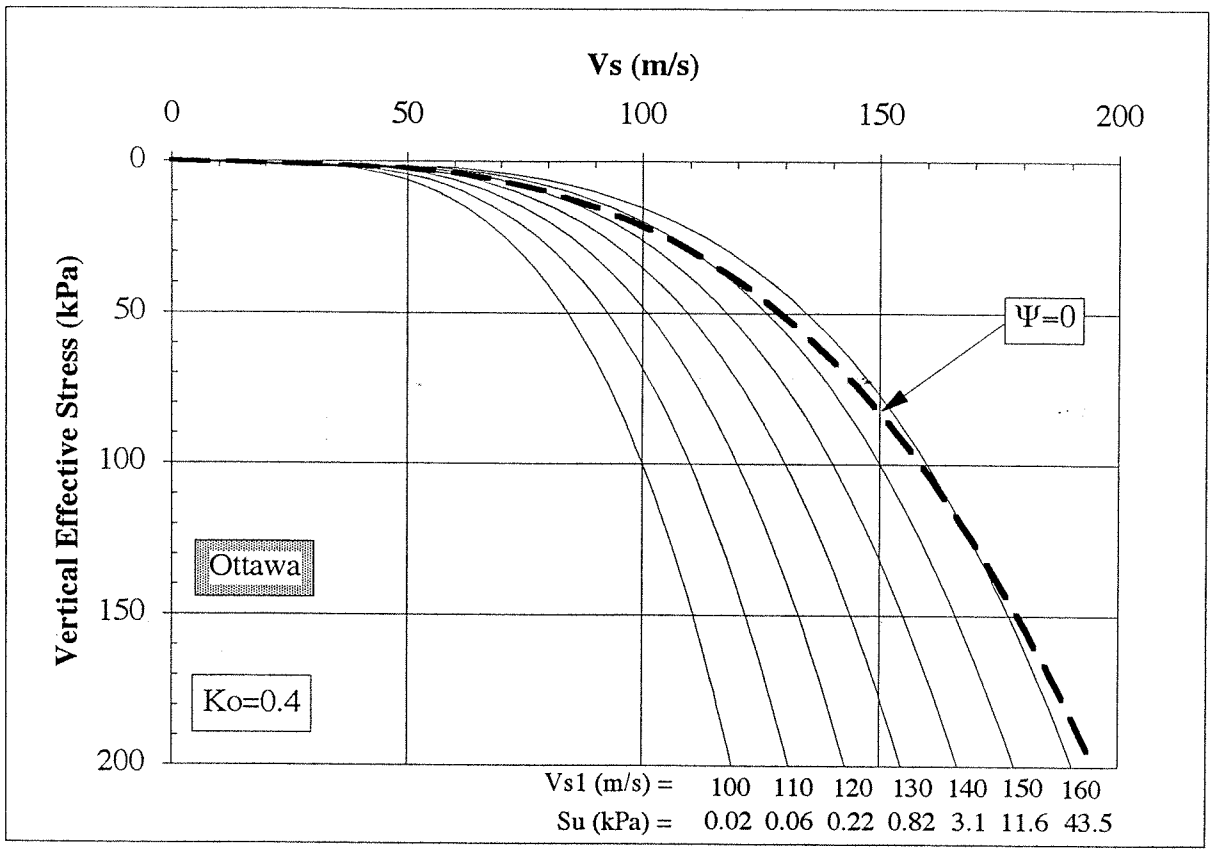

(b)

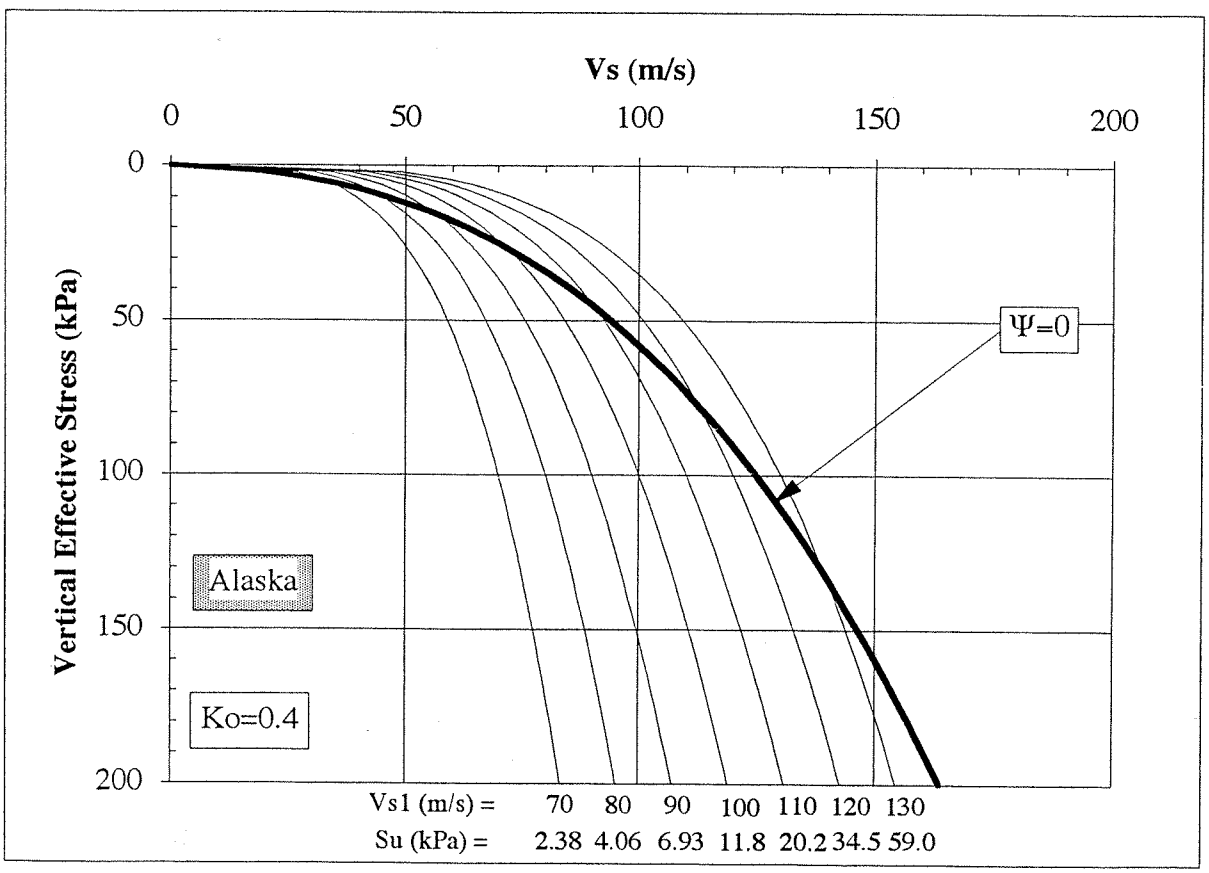

FIGURE 4 (a) & (b)

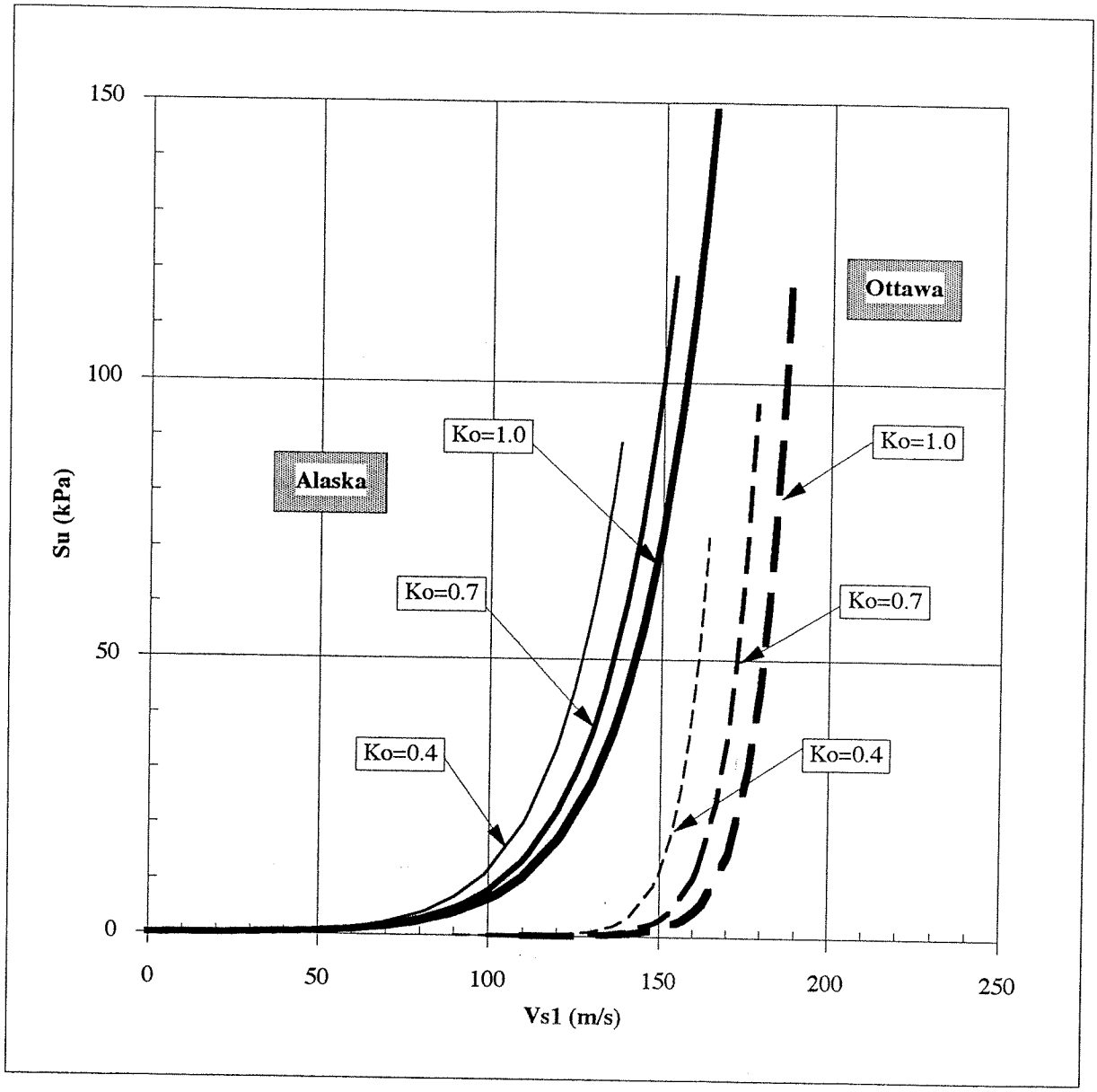
150
100
50
0
Su (kPa)
0
50
100
150
200
250
Vs1 (m/s)
Alaska
Ottawa
Ko=1.0
Ko=0.7
Ko=0.4
Ko=1.0
Ko=0.7
Ko=0.4

FIGURE 5

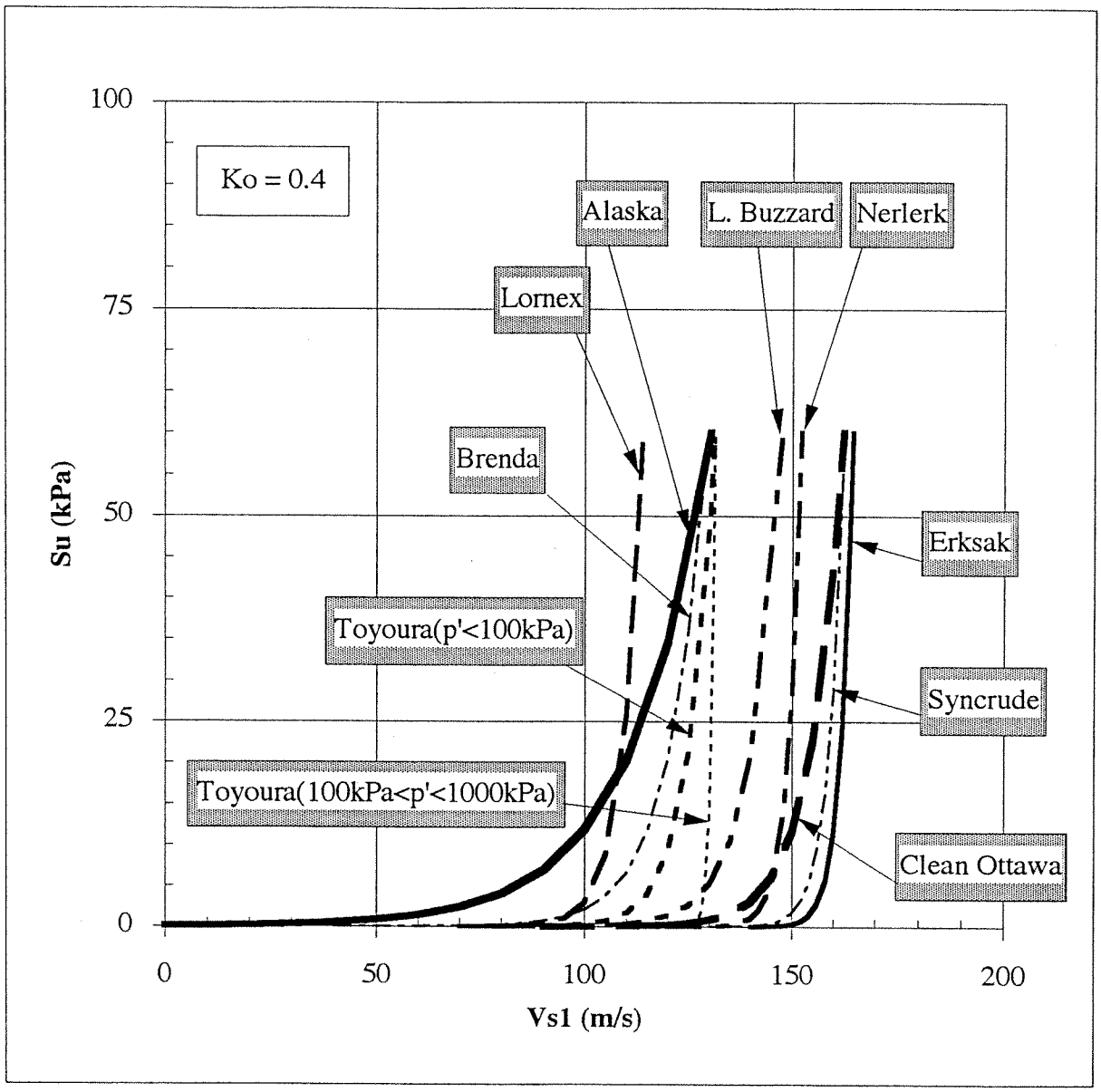
Ko = 0.4
Alaska
L. Buzzard
Nerlerk
Lornex
Brenda
Erksak
Toyoura(p'<100kPa)
Syncrude
Toyoura(100kPa<p'<1000kPa)
Clean Ottawa
Su (kPa)
Vs1 (m/s)
0
25
50
75
100
0
50
100
150
200

FIGURE 6

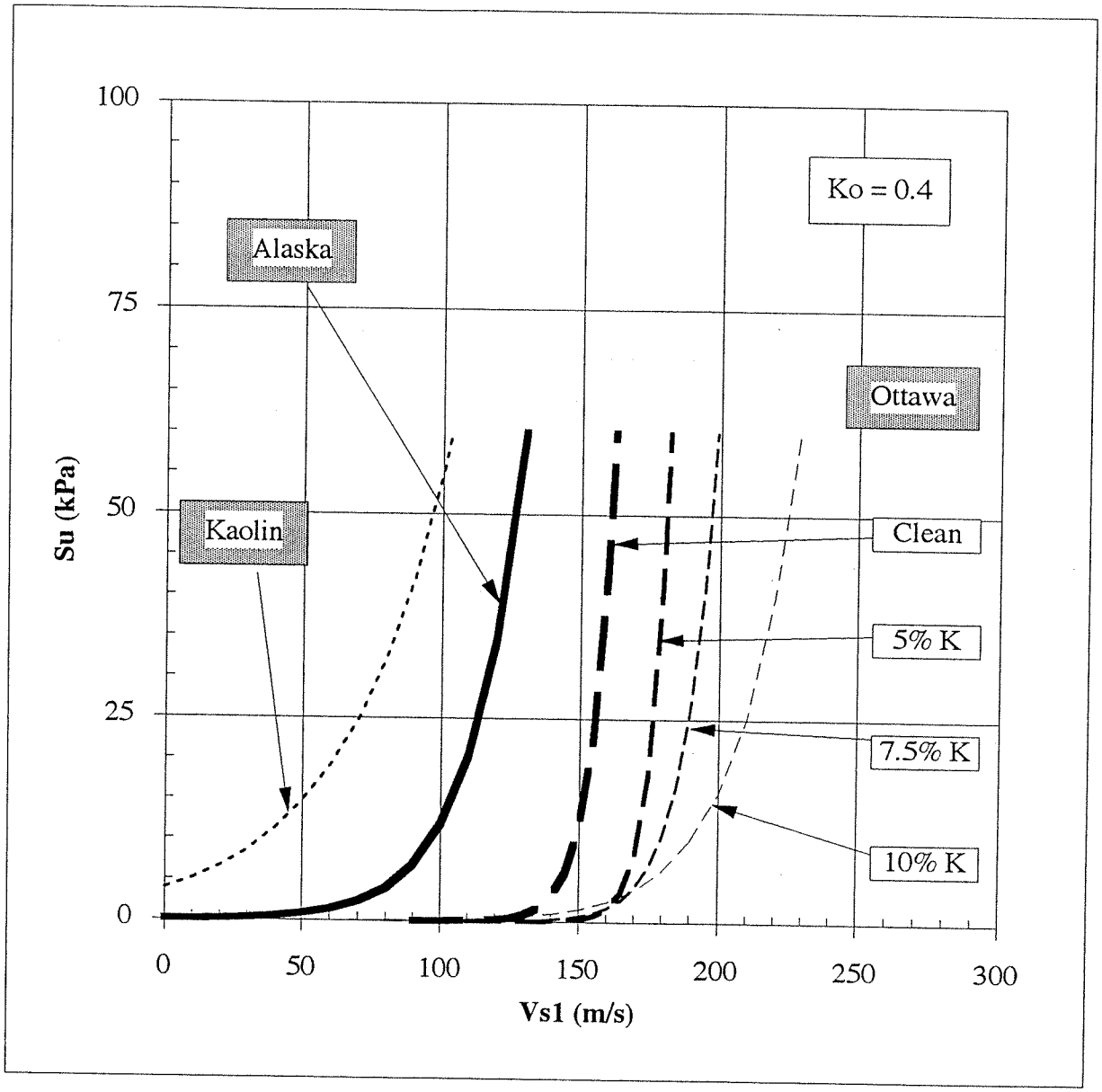
100
75
50
25
0
Su (kPa)
0
50
100
150
200
250
300
Vs1 (m/s)
Ko = 0.4
Alaska
Ottawa
Kaolin
Clean
5% K
7.5% K
10% K

FIGURE 7

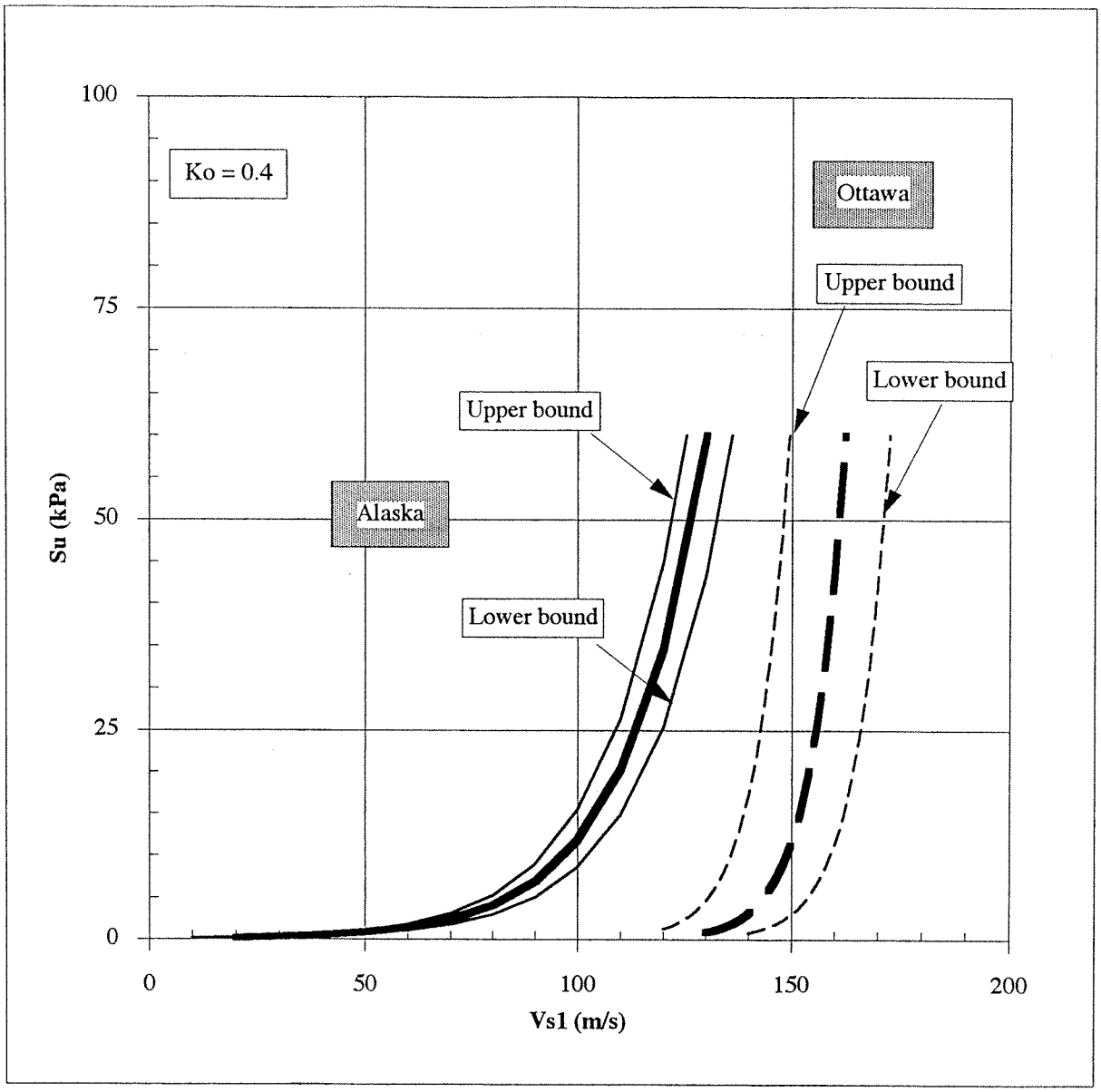
Ko = 0.4
Ottawa
Upper bound
Lower bound
Upper bound
Alaska
Lower bound
Su (kPa)
Vs1 (m/s)
100
75
50
25
0
0
50
100
150
200

FIGURE 8

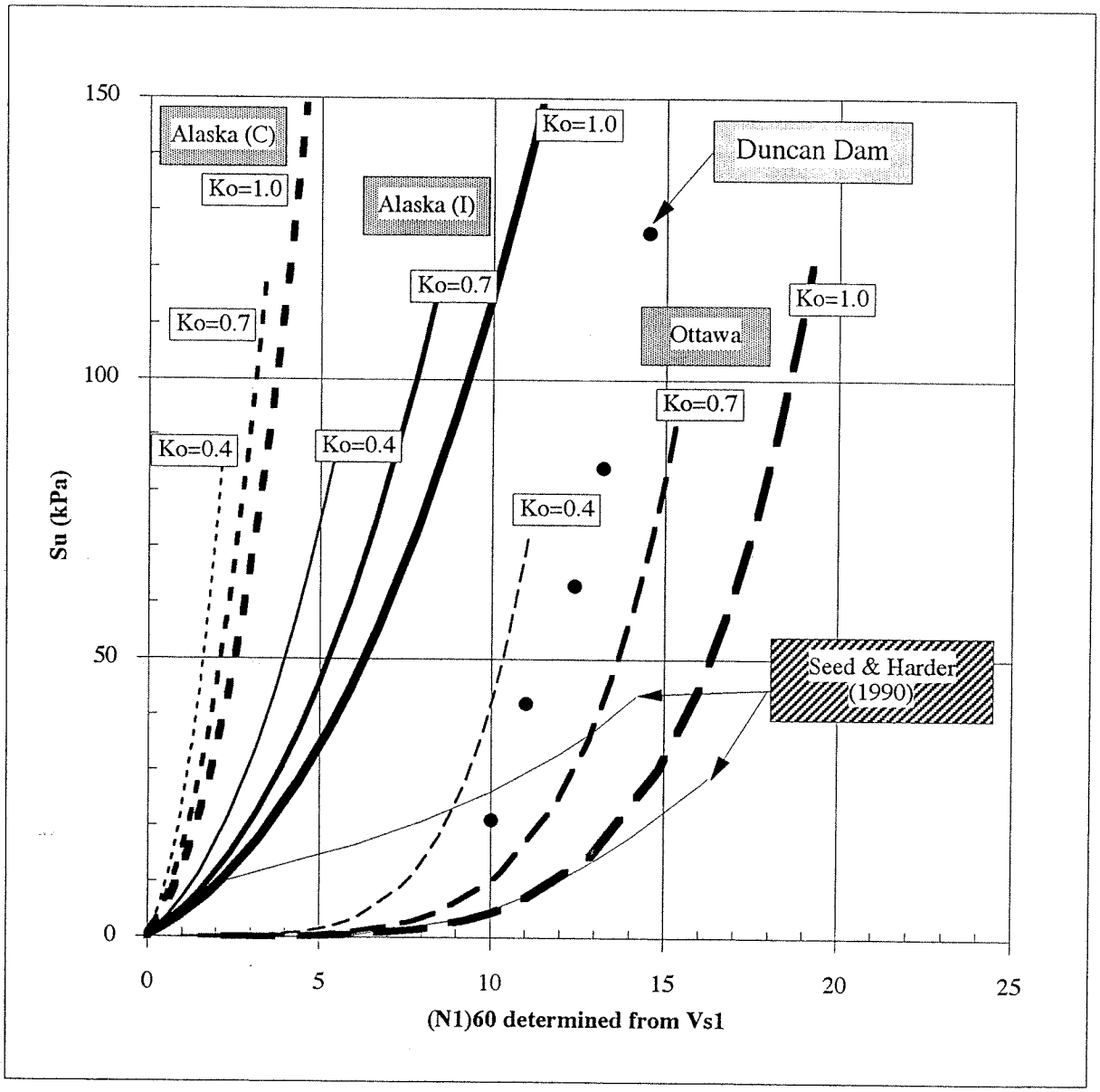
150
100
50
0
Su (kPa)
0
5
10
15
20
25
(N1)60 determined from Vs1
Alaska (C)
Ko=1.0
Ko=0.7
Ko=0.4
Alaska (I)
Ko=1.0
Ko=0.7
Ko=0.4
Duncan Dam
Ottawa
Ko=1.0
Ko=0.7
Ko=0.4
Seed & Harder (1990)

FIGURE 9

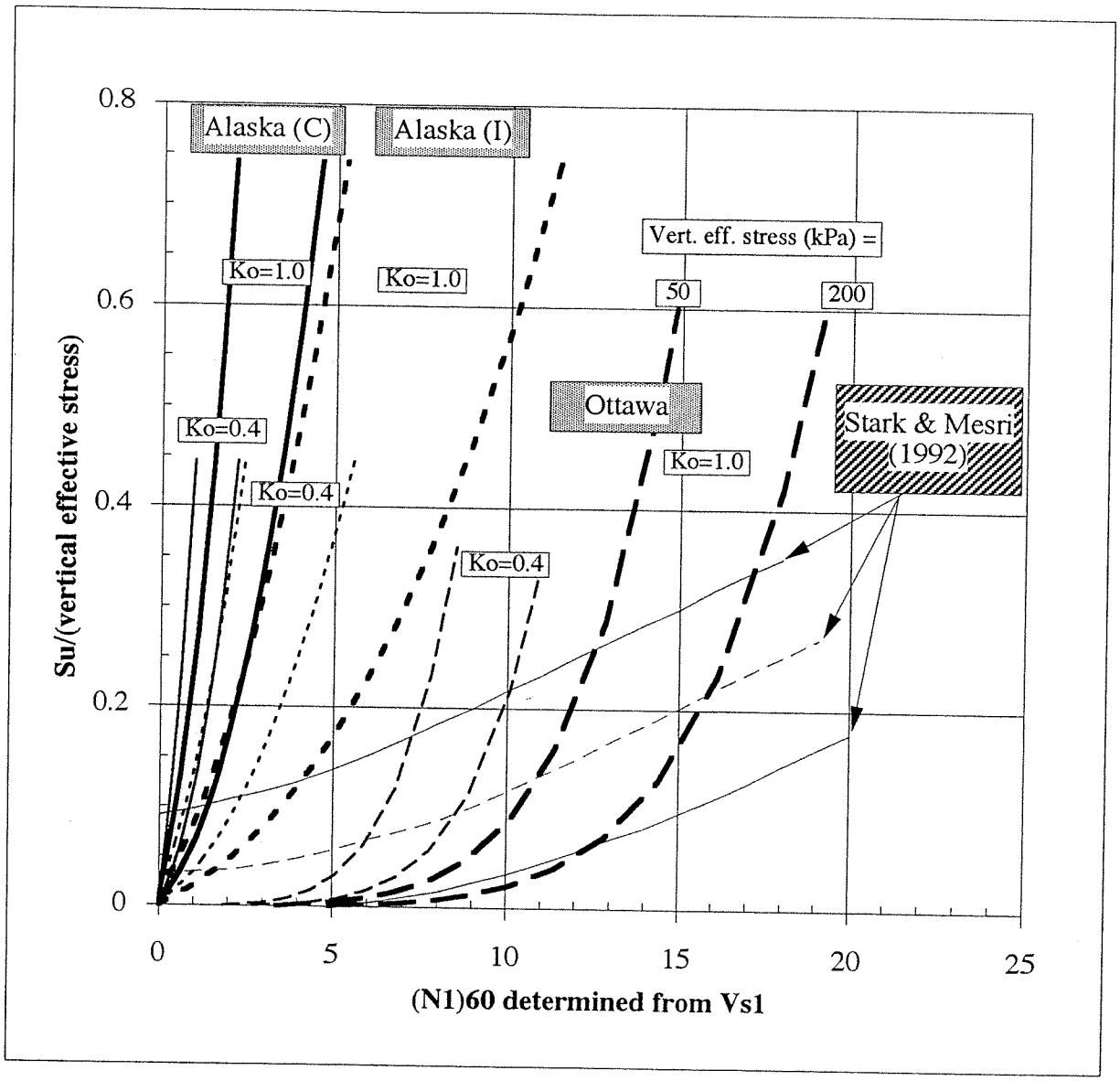
Alaska (C)
Alaska (I)
Ko=1.0
Ko=1.0
Ko=0.4
Ko=0.4
Ko=0.4
Vert. eff. stress (kPa) =
50
200
Ottawa
Ko=1.0
Stark & Mesri (1992)
Su/(vertical effective stress)
0.8
0.6
0.4
0.2
0
0
5
10
15
20
25
(N1)60 determined from Vs1

FIGURE 10

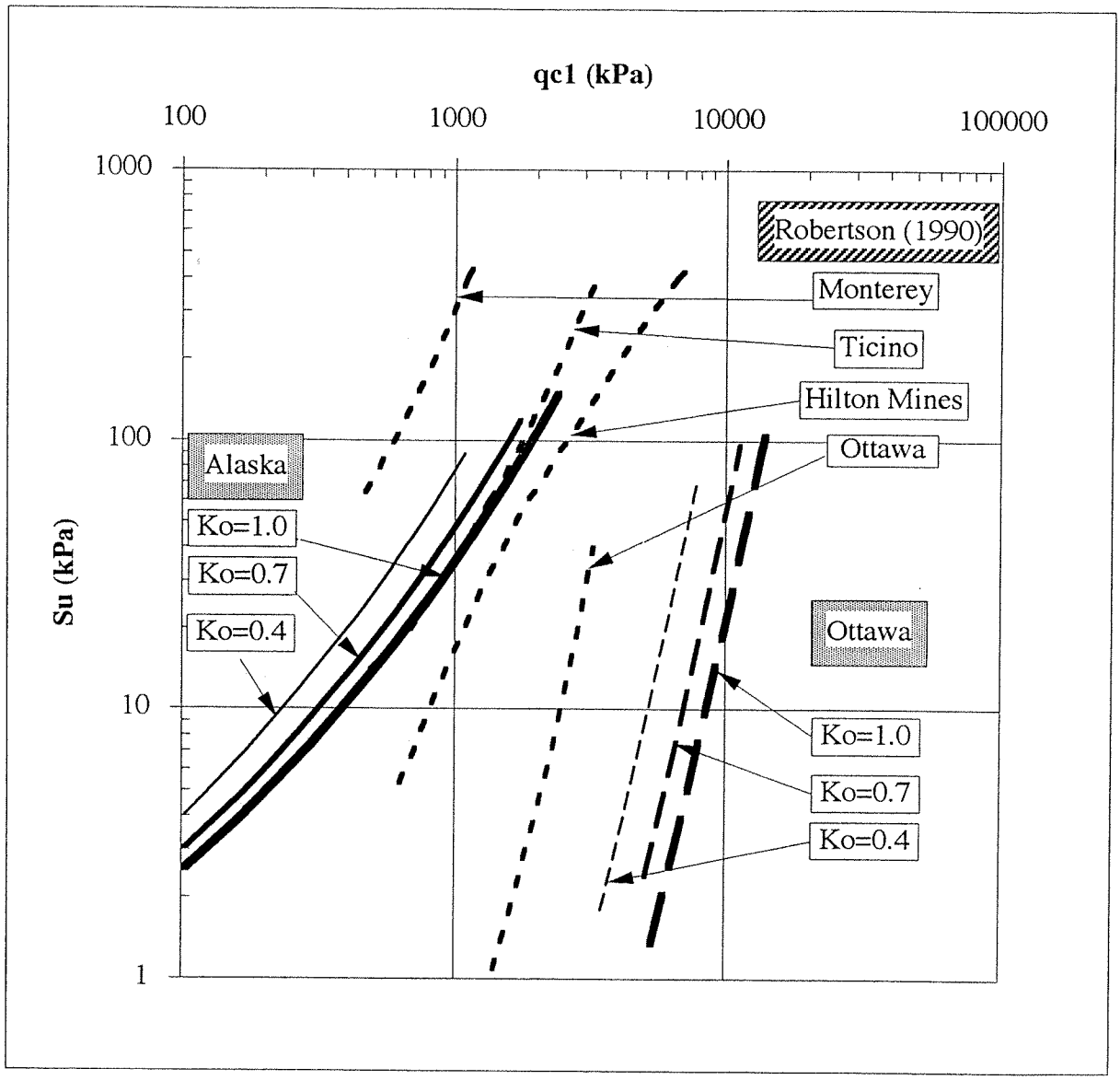
qc1 (kPa)
100
1000
10000
100000
1000
100
10
1
Su (kPa)
Robertson (1990)
Monterey
Ticino
Hilton Mines
Ottawa
Alaska
Ko=1.0
Ko=0.7
Ko=0.4
Ottawa
Ko=1.0
Ko=0.7
Ko=0.4

FIGURE 11

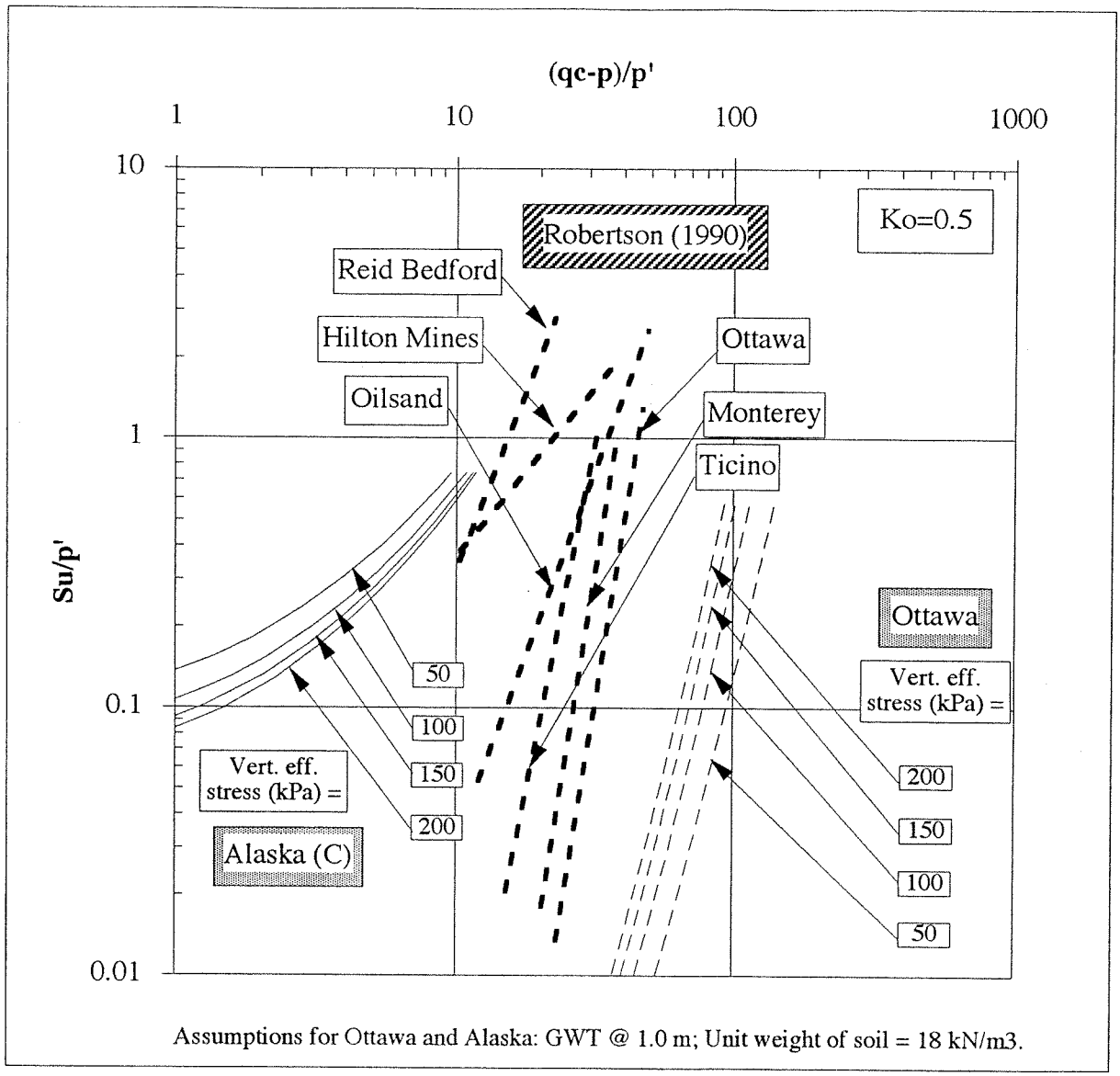

Assumptions for Ottawa and Alaska: GWT @ 1.0 m; Unit weight of soil = 18 kN/m3.

FIGURE 12